

Price Impact of Order Flow Imbalances: Multi-level, Cross-asset and Forecasting

Rama Cont¹, Mihai Cucuringu^{1, 2, 3}, and Chao Zhang²

¹Mathematical Institute, University of Oxford, Oxford, UK

²Department of Statistics, University of Oxford, Oxford, UK

³The Alan Turing Institute, London, UK

January 2022

Abstract

We investigate the impact of order flow imbalance (OFI) on price movements in equity markets in a multi-asset setting. First, we show that taking into account multiple levels of the order book when defining order book imbalance leads to higher explanatory power for the contemporaneous **price impact** of OFI. Using a principal component analysis of OFI across order book levels, we define a notion of *integrated OFI* which shows superior explanatory power for market impact both in-sample and out-of-sample.

Second, we examine the notion of **cross-impact** and show that, once the information from multiple levels is included in OFI, multi-asset models with cross-impact do not provide additional explanatory power for contemporaneous impact compared to a sparse model without cross-impact terms. However, we find evidence that cross-impact terms provide additional information for intraday forecasting of future returns.

Keywords: Order flow imbalance; Price impact; Cross impact; LASSO; principal component analysis; Return prediction.

JEL Codes: C31, C53, G17

1 Introduction

Price dynamics in most major stock exchanges are driven by the intraday flow of buy and sell orders through a centralized limit order book, as shown in Figure 1. While early studies on market impact focused on the impact of trade imbalances arising from market orders (e.g. [12]), empirical studies on intraday data have identified the Order Flow Imbalance (OFI), defined as the net order flow resulting from the imbalance buy and sell orders [17, 11, 52], as the main driver of price changes. A number of studies [11, 49] explore the role of OFI in cross-impact. Some related literature will be reviewed briefly in the corresponding section.

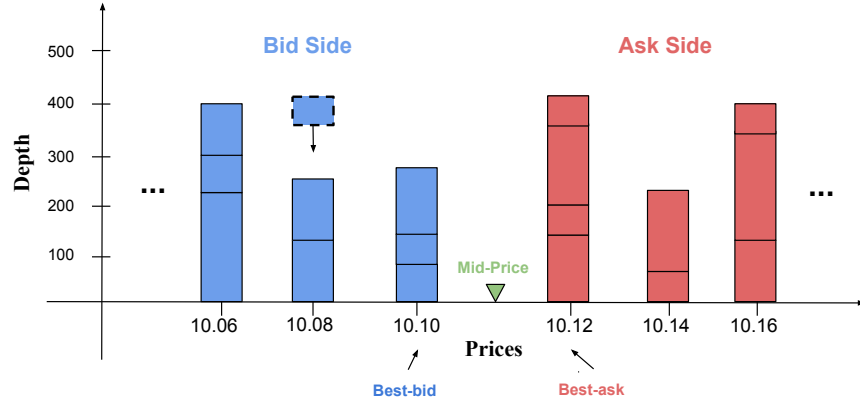


Figure 1: Illustration of a limit order book (LOB), with three levels for each of the bid and ask sides.

In the present paper we systematically examine the impact of order flow imbalances on *contemporaneous price impact, contemporaneous cross-impact and forecasting of future returns*.

Price impact on contemporaneous returns. First, we show that taking into account multiple levels of the order book when defining order book imbalance leads to higher explanatory power for the contemporaneous price impact of OFI. Our empirical evidence shows that, as OFIs at deeper order book levels are included as features, the explained percentage of variance steadily increases in the in-sample tests. Using a principal component analysis of OFI across order book levels, we observe that the first principal component of multi-level OFIs can explain more than 80% of the total variance. Based on these results, we define a notion of *integrated OFI* which shows superior explanatory power for price impact over best-level OFIs and multi-level OFIs in both in-sample and out-of-sample. It is worth emphasizing that we use both in-sample and out-of-sample tests to assess the model’s performance, while previous works [17, 11] only focus on in-sample tests.

Contemporaneous cross impact. An important question concerns the existence of cross-impact, i.e. assessing whether one stock’s prices/returns are influenced by the order flow imbalances of other stocks (see

[7, 11, 44]). Recently, Capponi and Cont [11] proposed a procedure to distinguish the impact of common and idiosyncratic factors in order flow using conditional regressions. Their results show that in many cases "cross-impact" coefficients are not statistically significant and cross-impact is in fact a manifestation of common components in order flow.

We revisit this question with an approach which takes into account model sparsity, using the Least Absolute Shrinkage and Selection Operator (LASSO) to estimate a linear model of contemporaneous impact with self- and cross-impact terms. By comparing with the price impact model using best-level OFIs, we find that the cross-impact model using the best-level OFIs of multiple assets as candidate features can provide small but significant additional explanatory power for price movements. Moreover, our results show that, once the information from multiple levels is included in OFI, multi-asset models with cross-impact do not provide additional explanatory power for contemporaneous impact compared to a sparse model without cross-impact terms. These findings suggest that consolidating multi-level OFIs, such as our integrated OFIs, is a more effective method to model price dynamics than introducing cross-impact terms. To the best of our knowledge, this is the first study to comprehensively analyze the relations between contemporaneous individual returns and multi-level order flow imbalances of individual or multiple stocks.

Forecasting future returns. Finally, we investigate the use of OFI to forecast future returns. We study a multiperiod price-impact model using lagged OFIs to predict returns and find evidence that cross-impact terms provide additional information for intraday forecasting of future returns.

Our contributions may be summarized as follows:

1. We show that order flow at deeper levels of the limit order books provides additional explanatory power for price impact, when compared to the order flow imbalance at the best-level.
2. We provide a systematic approach for combining OFIs at the top levels of the book into an integrated OFI variable which best explains price impact.
3. We show evidence that there is no need to introduce cross-impact terms for modeling the contemporaneous returns, as long as the OFI incorporates information from multiple levels, not just the best level.
4. Cross-asset OFIs improve the forecast of future returns, thus providing evidence of cross-impact in the forward-looking model.

Paper outline. The remainder of this paper is structured as follows. In Section 2, we establish the notations and terminology employed throughout the paper. Section 3 presents studies about the price-impact model on contemporaneous returns. Section 4 turns to the cross-impact model on contemporaneous returns. In Section 5, we first discuss the forward-looking versions of the price-impact and cross-impact models, and then examine the economic gains from forecast returns. Finally, we conclude our analysis in Section 6 and highlight potential future research directions.

2 Notation

We first establish notations for various quantities used throughout the paper.

Best-level OFI. We use the following definition of OFI (proposed by Cont et al. [17]) in our analysis

$$\text{OFI}_{i,t}^{1,(h)} := \sum_{n=N(t-h)+1}^{N(t)} q_{i,n}^{1,b} 1_{\{P_{i,n}^{1,b} \geq P_{i,n-1}^{1,b}\}} - q_{i,n-1}^{1,b} 1_{\{P_{i,n}^{1,b} \leq P_{i,n-1}^{1,b}\}} - q_{i,n}^{1,s} 1_{\{P_{i,n}^{1,s} \leq P_{i,n-1}^{1,s}\}} + q_{i,n-1}^{1,s} 1_{\{P_{i,n}^{1,s} \geq P_{i,n-1}^{1,s}\}}. \quad (1)$$

Here, $P_{i,n}^{1,b}$ and $q_{i,n}^{1,b}$ denote the best bid price and size (in number of shares) of stock i , respectively. Similarly, $P_{i,n}^{1,s}$ and $q_{i,n}^{1,s}$ denote the ask price and ask size at the best level, respectively. We enumerate the observations of the bid and the ask by n , and $N(t-h)+1$ and $N(h)$ are the index of the first and the last order book event in the interval $(t-h, t]$. Thus $\text{OFI}_{i,t}^{1,(h)}$ calculates the accumulative order flow imbalances at the best bid/ask side during the time interval $(t-h, t]$, where h denotes the horizon. Note that the variable $\text{OFI}_{i,t}^{1,(h)}$ increases when

- the bid size increases and the best bid price remains the same;
- the ask size decreases and the best ask price remains the same;
- the best bid/ask prices increase.

One can perform an analogous analysis for the decreasing case.

Deeper-level OFI. A natural extension of the best-level OFI defined in Eqn (1) is deeper-level OFI. We define OFI at level m ($m \geq 1$) as follows

$$\text{OFI}_{i,t}^{m,(h)} := \sum_{n=N(t-h)+1}^{N(t)} q_{i,n}^{m,b} 1_{\{P_{i,n}^{m,b} \geq P_{i,n-1}^{m,b}\}} - q_{i,n-1}^{m,b} 1_{\{P_{i,n}^{m,b} \leq P_{i,n-1}^{m,b}\}} - q_{i,n}^{m,s} 1_{\{P_{i,n}^{m,s} \leq P_{i,n-1}^{m,s}\}} + q_{i,n-1}^{m,s} 1_{\{P_{i,n}^{m,s} \geq P_{i,n-1}^{m,s}\}}. \quad (2)$$

Here, $P_{i,n}^{m,b}$ and $q_{i,n}^{m,b}$ denote, respectively, the bid price and bid size (in number of shares) at level m of the order book. Similarly, $P_{i,n}^{m,s}$ and $q_{i,n}^{m,s}$ denote the ask price and ask size at level m .

Normalized OFI. Due to the intraday pattern in limit order depth [2], we use the average size [27] to scale OFI at the corresponding level.

$$\text{ofi}_{i,t}^{m,(h)} = \frac{\text{OFI}_{i,t}^{m,(h)}}{Q_{i,t}^{M,(h)}}, \quad (3)$$

where $Q_{i,t}^{M,(h)} = \sum_{m=1}^M \frac{1}{2\Delta N(t)} \sum_{t=N(t-h)+1}^{N(t)} [q_{i,n}^{m,b} + q_{i,n}^{m,s}]$ is the sum order book depth across the first M levels and $\Delta N(t) = N(t) - N(t-h)$ is the number of events during $(t-h, t]$. Throughout the paper, we use the first $M = 10$ levels.

Logarithmic return. We denote the logarithmic return of asset i during $(t-h, t]$ by

$$R_{i,t}^{(h)} = \log \left(\frac{P_{i,t}}{P_{i,t-h}} \right), \quad (4)$$

where $P_{i,t}$ is the mid-price at time t , i.e. $P_{i,t} = \frac{P_{i,t}^{1,b} + P_{i,t}^{1,s}}{2}$.

Normalized return. Taking into account the fact that the intraday pattern in price volatility has been extensively demonstrated [41, 17, 24], we normalize $R_{i,t}^{(h)}$ by its historical volatility and denote $r_{i,t}$ as the normalized return.

$$r_{i,t}^{(h)} = \frac{R_{i,t}^{(h)}}{\sigma_{i,t} \sqrt{h}}, \quad (5)$$

where $\sigma_{i,t}$ is the average value of standard deviations of minutely returns during $[t-30, t]$, across the previous five trading days.

3 Price impact

In this section, we study the price-impact model using LOB data. We first compare the effects of best-level OFIs with multi-level OFIs. Due to the redundancy of information across multi-level OFIs, we propose an integrated version of OFIs, and evaluate its efficacy on modeling price changes.

3.1 Related literature

The relationship between contemporaneous order flow imbalance and price movement, also known as price-impact (see Bouchaud [8], Cont et al. [17], Lillo et al. [40]), has drawn substantial attention in recent decades, due to its importance for studying price dynamics. On the other hand, price impact model is relevant to some practical problems, e.g. estimating trading costs (see Frazzini et al. [22]) and devising optimal execution models (see Guo and Zervos [26]).

A series of previous studies mainly focus on the impact of imbalances between buy and sell market orders. Taranto et al. [47] propose a framework aiming to build a precise linear model of price dynamics based on two types of market orders: (1) those that leave the price unchanged, and (2) those which lead to an immediate price change. Brown et al. [9] adopt a bivariate vector auto-regression (VAR) to study the interaction between order imbalance and stock return. Using data from the Australian Stock Exchange, the authors conduct causality tests and observe a strong bi-directional contemporaneous relationship. Instead of modeling the temporary impact, Eisler et al. [20] empirically analyze the impact of different order events on future price changes.

The literature regarding the impact of limit orders includes the following works, that are more relevant to our present study. Cont et al. [17] use a linear model to describe the contemporaneous impact of the order flow imbalance on price dynamics. Their proposed measure, order flow imbalance, is built on the following order book events: limit orders, market orders, and cancellations. There is substantial evidence on the significant relationship between the order flow imbalance and price changes. However, Cont et al. [17] only investigate the in-sample R^2 and ignore the generalization error of their regressions. Xu et al. [52] extend the model of [17] to multi-level order flow imbalance. They argue that even though strong correlations exist between the net order flow at different price levels, multi-level limit orders are still statistically informative. Furthermore, Xu et al. [52] adopt a cross-validation method to estimate the out-of-sample root-mean-square error; however, they do not preserve the chronological order of the data, and their experiments are performed on only six stocks for one year of data. In contrast, in our study, we obey the temporal ordering of the data, and our study is based on around 100 stocks over three years of data.

3.2 Models for Price-impact

Price-impact of best-level OFIs. We first pay attention to the impact of best-level OFIs, i.e. $\text{ofi}_{i,t}^{1,(h)}$ on **contemporaneous returns** $r_{i,t}^{(h)}$, which materialize over the same time bucket as the OFI.

$$\text{PI}^{[1]} : \quad r_{i,t}^{(h)} = \alpha_i^{[1]} + \beta_i^{[1]} \text{ofi}_{i,t}^{1,(h)} + \epsilon_{i,t}^{[1]}. \quad (6)$$

Here, $\epsilon_{i,t}^{[1]}$ is a noise term summarizing the influences of other factors, such as the order flow imbalances at deeper levels, and potentially the trading behaviours of other stocks. For the sake of simplicity, we denote the above regression model as $\text{PI}^{[1]}$, and use ordinary least squares (OLS) to estimate it.

Price-impact of multi-level OFIs. We then perform an extended version of $\text{PI}^{[1]}$ using multi-level OFIs as features in the model,

$$\text{PI}^{[m]} : \quad r_{i,t}^{(h)} = \alpha_i^{[m]} + \sum_{k=1}^m \beta_i^{[m],k} \text{ofi}_{i,t}^{k,(h)} + \epsilon_{i,t}^{[m]}. \quad (7)$$

Recall that $\text{ofi}_{i,t}^{k,(h)}$ is the normalized OFIs at level k . We refer to this model as $\text{PI}^{[m]}$, and use OLS to estimate it.

Principal Components Analysis (PCA) is a widely-used statistical procedure that applies an orthogonal transformation to convert a set of possibly correlated variables into a smaller number of uncorrelated variables (see Jolliffe and Cadima [34], Wold et al. [50]). The main objective of PCA is to determine the important directions which can explain most of the original variability in the data. PCA projects data onto these important directions, thus reduces the dimensionality of data. For example, we can drop the eigenvectors with the lowest eigenvalues due to their low information content. As a result, PCA can be employed to capture dominant factors driving the market (e.g. Jolliffe [33], Avellaneda and Lee [4]).

In general, PCA entails the following steps: 1. computing the covariance/correlation matrix; 2. computing eigenvalues and eigenvectors; 3. sorting eigenvalues and identifying principal components; 4. interpreting the results. More specifically, assume the data is given by the random vector $\mathbf{x} = (x_1, \dots, x_p)^\top \in \mathbb{R}^p$. If we have n observations $\{\mathbf{x}^{(i)}\}_{i=1}^n$ of \mathbf{x} , we can construct the sample matrix, denoted as $\mathbf{X} = [\mathbf{x}^{(1)}, \dots, \mathbf{x}^{(n)}]^\top \in \mathbb{R}^{n \times p}$. Next, we compute the empirical covariance matrix of \mathbf{x} by

$$\mathbf{S} = \frac{1}{n-1} (\mathbf{X} - \bar{\mathbf{x}})^\top (\mathbf{X} - \bar{\mathbf{x}}), \quad (8)$$

where $\bar{\mathbf{x}} = \frac{1}{n} \sum_{i=1}^n \mathbf{x}^{(i)}$ is the empirical mean vector.

In order to maximize the variance of the projected variable, the principal vectors $\{\mathbf{w}_k\}_{k=1}^p$ and their associated eigenvalues $\{\lambda_k\}_{k=1}^p$ have to satisfy

$$\begin{aligned} \mathbf{w}_k &= \arg \max_{\mathbf{w} \in \mathbb{R}^p} \{ \mathbf{w}^\top \mathbf{S} \mathbf{w} : \mathbf{w}^\top \mathbf{w}_j = 0, \forall 1 \leq j < k, \|\mathbf{w}\|_2 = 1 \}, \\ \lambda_k &= \max_{\mathbf{w} \in \mathbb{R}^p} \{ \mathbf{w}^\top \mathbf{S} \mathbf{w} : \mathbf{w}^\top \mathbf{w}_j = 0, \forall 1 \leq j < k, \|\mathbf{w}\|_2 = 1 \}. \end{aligned} \quad (9)$$

Price-impact of Integrated OFIs. In order to make use of the information embedded in multiple LOB levels and avoid overfitting, we propose an integrated version of OFIs, as shown in Eqn (10), which only preserves the first principal component. We further normalize the first principal component by dividing by its l_1 norm so that the weights of multi-level OFIs in constructing integrated OFIs sum to 1. Specifically, denoting the multi-level OFI vector as $\text{ofi}_{i,t}^{(h)} = (\text{ofi}_{i,t}^{1,(h)}, \dots, \text{ofi}_{i,t}^{10,(h)})^\top$, we consider the following measure as the integrated OFI,

$$\text{ofi}_{i,t}^{I,(h)} = \frac{\mathbf{w}_1^\top \text{ofi}_{i,t}^{(h)}}{\|\mathbf{w}_1\|_1}, \quad (10)$$

where \mathbf{w}_1 is the first principal vector computed from historical data. To the best of our knowledge, this is the first work to *aggregate multi-level OFIs into a single variable*.

In practice, we use samples of $\mathbf{ofi}_{i,s}^{(h)}$ during the previous 30 minutes, $s \in [t - 30, t)$, to compute the principal components. Then we apply the first principal vector to transform the multi-level OFI vector $\mathbf{ofi}_{i,t}^{(h)}$ to $\mathbf{ofi}_{i,t}^{I,(h)}$. For example, if using minutely buckets, we perform PCA on a matrix of size 30×10 . For 10-second buckets, the PCA input matrix is of size 180×10 , since there are 180 buckets of 10-second length in a 30-minute interval.

Finally, we estimate the impact of $\mathbf{ofi}_{i,t}^{I,(h)}$ on the returns, and denote this model as PI^I .

$$\text{PI}^I : \quad r_{i,t}^{(h)} = \alpha_i^I + \beta_i^I \mathbf{ofi}_{i,t}^{I,(h)} + \epsilon_{i,t}^I. \quad (11)$$

3.3 Empirical results

Data. We use the Nasdaq ITCH data from LOBSTER¹ to compute OFIs and returns during the intraday time interval 10:00AM-3:30PM. The reason for excluding the first and last 30 minutes of the trading day is due to the increased volatility near the opening and closing session (see [28, 14, 15]). Our data includes the top 100 components of S&P500 index, for the period 2017-01-01 to 2019-12-31.

Implementation. For a more representative and fair comparison with previous studies [17, 52], we apply the same procedure described in Cont et al. [17] to our experiments. That is, we use a 30-minute estimation window and within each window, returns and OFIs are computed for every 10 seconds, i.e. $h = 10$ seconds. Altogether, this amounts to $30 \times 60 / 10 = 180$ observations for each regression.

Performance evaluation. We use the past 30-minute data to fit the above regressions, namely Eqns (6), (7), and (11). We then calculate their adjusted- R^2 , denoted as the **in-sample** R^2 (or **IS** R^2). In order to assess how well the model generalizes to unseen data, we propose to perform the following out-of-sample tests. We use the fitted model to estimate returns on the following 30-minute data and compute the corresponding R^2 , denoted as the **out-of-sample** R^2 (or **OOS** R^2). Because we drop the first and last half-hour of each trading day from our samples and perform out-of-sample tests, this leads to 10 linear regressions contained in each trading day for a given stock.

Price-impact of multi-level OFIs. From Table 1, we observe that $\text{PI}^{[1]}$ can explain 71.16% of the in-sample variation of a stock's contemporaneous returns. In terms of out-of-sample data, $\text{PI}^{[1]}$ can explain 64.64% of returns' variation.

¹<https://lobsterdata.com/>

		PI ^[1]	PI ^[2]	PI ^[3]	PI ^[4]	PI ^[5]	PI ^[6]	PI ^[7]	PI ^[8]	PI ^[9]	PI ^[10]
In-Sample	R^2 (%)	71.16	81.61	85.07	86.69	87.66	88.30	88.74	89.04	89.24	89.38
	ΔR^2 (%)		10.45	3.46	1.62	0.97	0.64	0.44	0.30	0.20	0.14
	<i>p</i> -Value		0.00	0.00	0.00	0.00	0.00	0.00	0.00	0.00	0.00
Out-Of-Sample	R^2 (%)	64.64	75.81	79.47	81.13	82.05	82.65	83.01	83.16	83.15	83.11
	ΔR^2 (%)		11.17	3.66	1.66	0.92	0.60	0.36	0.15	-0.01	-0.04
	<i>p</i> -Value		0.00	0.00	0.00	0.00	0.00	0.00	0.51	0.93	

Table 1: Average adjusted- R^2 (in percentage points) of PI^[1] (Eqn (6)) and PI^[m] (Eqn (7)). The top and bottom panels report the results in in-sample and out-of-sample tests, respectively. ΔR^2 is the increase in adjusted- R^2 between PI^[m] and PI^[m+1] ($m = 1, \dots, 9$). The *p*-value represents the probability of observing the increase in adjusted- R^2 under the null hypothesis of no increase from PI^[m] to PI^[m+1] ($m = 1, \dots, 9$).

The top panel of Table 1 shows that the in-sample R^2 values increase as more multi-level OFIs are included as features, which is not surprising given that PI^[m] is a nested model of PI^[m+1]. However the increments of the in-sample R^2 are descending, indicating that much deeper LOB data might be unable to provide additional information. This argument is confirmed by the models' performance on out-of-sample data, as shown at the bottom panel of Table 1. Out-of-sample R^2 reaches a peak at PI^[8].

Impact comparison between multi-level OFIs. An interesting question is whether the OFIs at different price levels contribute evenly in terms of price impact. Based on Figure 2 (a), we conclude that multi-level OFIs have different contributions to price movements. Generally, ofi² (OFIs at the second-best level) reflects greater influence than ofi¹ (OFIs at the best level) in model PI^[10], which is perhaps counter-intuitive, at first sight.

We further investigate how the coefficients vary across stocks with different characteristics, such as volume, volatility, and bid-ask spread. Figure 2 (b)-(d) reveals that for stocks with *high-volume* and *small-spread*, order flow posted deeper in the LOB has more influence on price movements. The results regarding spread are in line with Xu et al. [52], where it is observed that for large-spread stocks (AMZN, TSLA, and NFLX), the coefficients of ofi^m tend to get smaller as the LOB level m increases, while for small-spread stocks (ORCL, CSCCO, and MU), the coefficients of ofi^m may become larger as m increases.

Cont et al. [17] conclude that the effect of ofi^m ($m \geq 2$) on price changes is only second-order or null. There are two likely causes for the differences between their findings and ours. First, the data used in Cont et al. [17] includes 50 stocks (randomly picked from S&P500 constituents) for a single month in 2010, while we use the top 100 large-cap stocks for 36 months during 2017-2019. Second, Cont et al. [17] consider the average of the coefficients across 50 stocks. In our work, we first group 100 stocks by firm characteristics, and then study the average coefficients of each subset. Therefore, our results are based on a more granular

analysis, across a significantly longer period of time.

Next, we investigate the correlations among multi-level OFIs. Figure 3 reveals that even though the correlation structure of multi-level OFIs may vary across stocks, they all show strong relationships (above 0.75). It is worth pointing out that the best-level OFI exhibits the smallest correlation with any of the remaining nine levels, a pattern which persists across the different stocks.

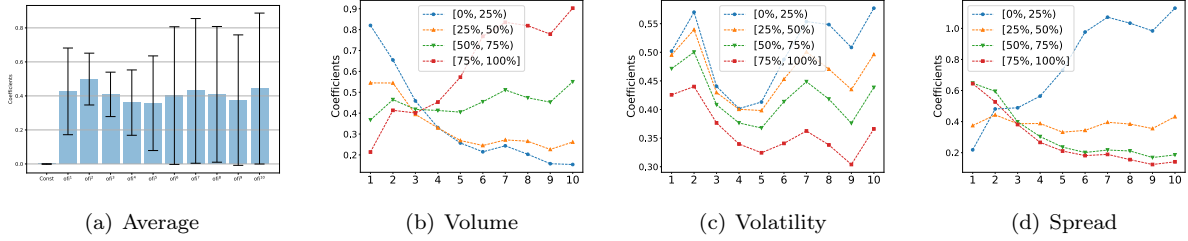


Figure 2: Coefficients of the model PI^[10]. (a) Average coefficients and one standard deviation (error bars), (b)-(d) coefficients sorted by stock characteristics. Volume: trading volume on the previous trading day. Volatility: volatility of one-minute returns during the previous trading day. Spread: average bid-ask spread during the previous trading day. [0%, 25%], respectively [75%, 100%], denote the subset of stocks with the lowest, respectively highest, 25% values for a given stock characteristic. The x -axis represents different levels of OFIs and y -axis represents the coefficients.

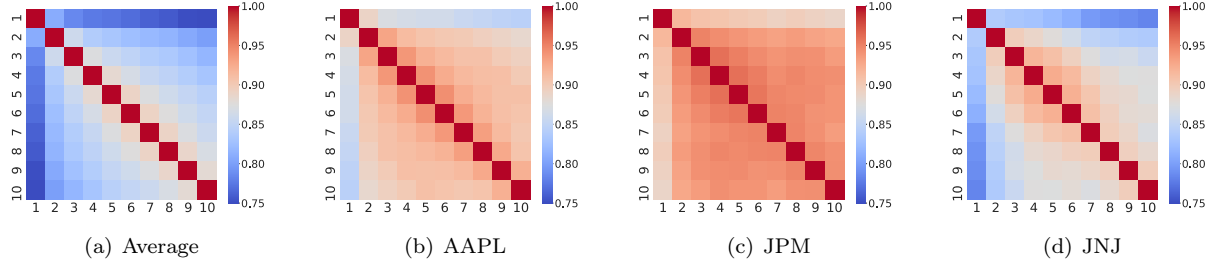


Figure 3: Correlation matrix of multi-level OFIs. (a) averaged across stocks, (b)-(d): correlation matrix of Apple (AAPL), JPMorgan Chase (JPM), and Johnson & Johnson (JNJ). The x -axis and y -axis represent different levels of OFIs.

Principal component of multi-level OFIs. Table 2 shows the average percentage of variance attributed to each principal component, and reveals that the first principal component explains more than 80% of the total variance. As a result, we create an integrated form of OFIs by projecting multi-level OFIs along the first principal component, as summarized in Eqn (10).

Principal Component	1	2	3	4	5	6	7	8	9	10
Explained Variance Ratio (%)	83.71	6.74	3.25	1.98	1.33	0.97	0.73	0.56	0.42	0.31

Table 2: Average percentage of variance attributed to each principal component, i.e. the ratio between the variance of each principal component and the total variance.

In Figure 4 we show statistics pertaining to the weights attributed to the 10 levels in the first principal component. Plot (a) shows the average weights, and the one standard deviation bars, across all stocks in the universe. In Figures (b-d), we plot the average principal component for three different stocks, where the average and one standard deviation bars are computed across buckets of time for a given stock. Figure 4 (a) reveals that the best-level OFI has the smallest weight in the first principal component, but the highest standard deviation, hinting that it fluctuates significantly across stocks. Altogether, Figures 3 and 4 provide evidence that stocks with different correlation structures of multi-level OFIs have different first principal component patterns. For example, for AAPL, its weight in the first component is increasing as the OFI goes deeper, whereas the weight in the first component of JPM peaks at the 6th level. Furthermore, Figure 5 shows various patterns for the first principal component of multi-level OFIs, for each quantile bucket of various stock characteristics, in particular, for volume, volatility and spread. For example, in Figure 5 (a), the red curve shows the average weights in the first principal component for each of the 10 levels, where the average is taken over all the top 25% largest volume stocks. A striking pattern that emerges from this figure is that for *high-volume*, and *low-volatility stocks*, OFIs deeper in the LOB receive more weight in the first component. However, for *low-volume*, and *large-spread stocks*, the best-level OFIs account more than the deeper-level OFIs.

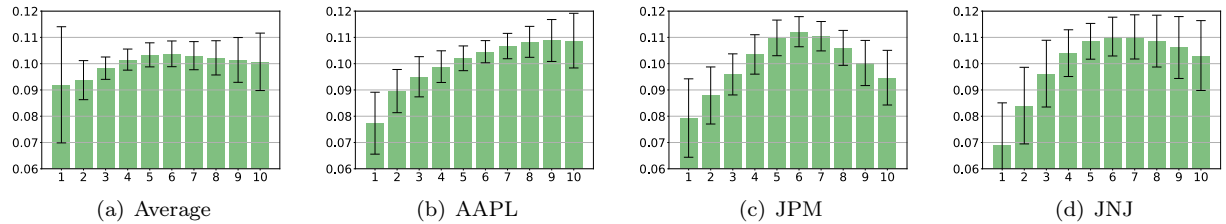


Figure 4: First principal component of multi-level OFIs. (a) averaged across stocks, (b)-(d): first principal component of Apple (AAPL), JPMorgan Chase (JPM), and Johnson & Johnson (JNJ). The x -axis represents different levels of OFIs and y -axis represents the weights of OFIs in the first principal component.

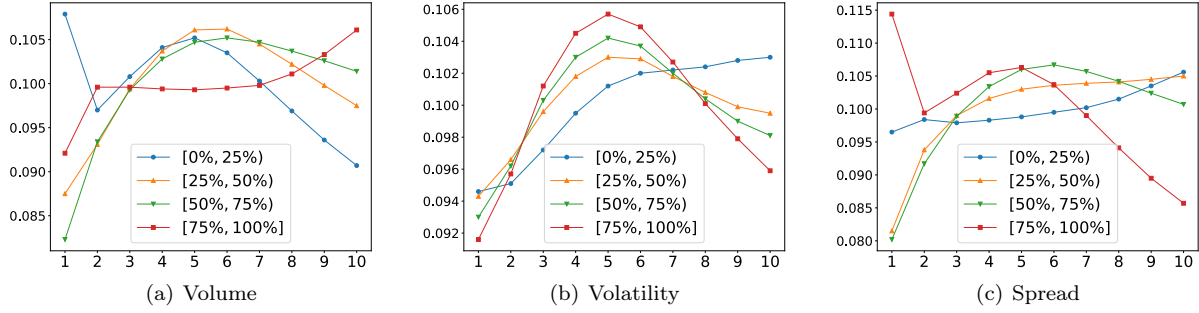


Figure 5: First principal component of multi-level OFIs, in quantile buckets for various stock characteristics. The x -axis indexes the top 10 levels of the OFIs. **Volume**: trading volume on the previous trading day. **Volatility**: volatility of one-minute returns during the previous trading day. **Spread**: average bid-ask spread during the previous trading day. $[0\%, 25\%]$, respectively $[75\%, 100\%]$, denote the subset of stocks with the lowest, respectively highest, 25% values for a given stock characteristic.

Performance of Integrated OFIs. Table 3 summarizes the relevant statistics of the price-impact model using integrated OFIs. Compared with Table 1, we observe that even though the in-sample R^2 of PI^I is lower than $\text{PI}^{[m]}$ (when $m \geq 5$), its performance in out-of-sample tests is better than $\text{PI}^{[m]} (\forall 1 \leq m \leq 10)$. It demonstrates the ability of PCA to extract information from the LOB data and reduce the chance of overfitting.

	PI^I
In-Sample R^2 (%)	87.14
Out-Of-Sample R^2 (%)	83.83

Table 3: This table presents the average results of PI^I (Eqn (11)). The first and second row report the adjusted R^2 in the in-sample and out-of-sample tests, respectively.

Time-series variation. Furthermore, we compare PI^I with $\text{PI}^{[m]}$ by month, as shown in Figure 6. For better readability, we only report the results when $m = \{1, 8\}$, that correspond to the most parsimonious model and the model with highest out-of-sample R^2 , respectively. To arrive at this figure, we average R^2 values in each month. Figure 6 reveals that the improvement of PI^I compared to $\text{PI}^{[1]}$ in the in-sample tests is consistent. In terms of out-of-sample tests, it is typically the case that the univariate regression PI^I can explain slightly more about price movements than the best multivariate regression, $\text{PI}^{[8]}$.

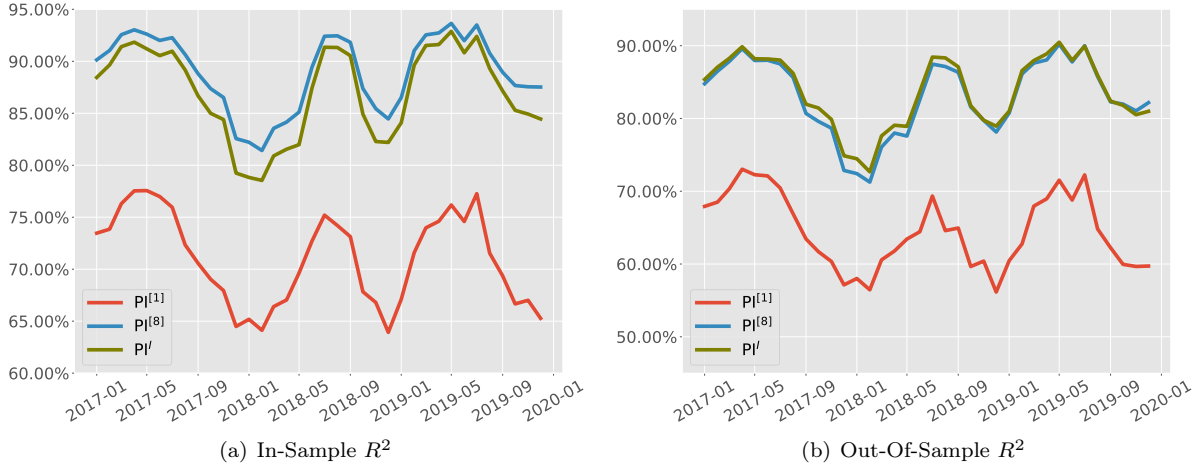


Figure 6: Time-series variation of R^2 by month, for different price-impact models. Panels (a) and (b) are based on the average results in the in-sample tests and out-of-sample tests, respectively.

Cross-sectional variation. Next, we ask the question whether the integrated OFIs affect stocks differently, depending on their characteristics. To this end, we report in Table 4 the results, both for in-sample and out-of-sample, for the best-level OFI and the integrated OFI, for each quartile bucket of the distribution obtained from the volume, volatility, and spread of the stocks in our universe. We conclude from Table 4 that the integrated OFIs can improve R^2 in price impact consistently across different subsets grouped by firm characteristics. Table 4 also shows that price-impact models can better explain *high-volume, low-volatility, and small-spread stocks*. These results shed new light on the modeling of price dynamics. Take spread as an example; for large-spread stocks, new orders are very likely to arrive inside the bid-ask spread as demonstrated by Xu et al. [52]. Now assume two limit buy orders, B_1 and B_2 (as depicted in Figure 7), have the same size but different prices; they will lead to the same multi-level OFI vectors but different mid-prices. Hence, it is more difficult to explain the impact of OFIs on prices for large-spread stocks. In terms of volatility and volume, a possible explanation may be due to their correlations with bid-ask spread. Previous studies (such as Abhyankar et al. [1], Wyart et al. [51]) found that there is a strong *positive* correlation between spread and volatility, while trading volume is *negatively* correlated with spread. For further studies on the price impact model, it is recommended to take these findings into account.

			[0%, 25%)	[25%, 50%)	[50%, 75%)	[75%, 100%)
ofi ¹	Volume	IS	57.02	70.87	77.11	80.43
		OOS	48.87	64.63	71.72	73.86
	Volatility	IS	73.25	72.24	70.81	67.67
		OOS	66.98	66.28	64.61	59.71
	Spread	IS	83.16	77.43	69.61	54.37
		OOS	77.39	71.84	63.64	45.37
ofi ^I	Volume	IS	70.24	86.27	92.97	96.31
		OOS	65.94	83.37	90.09	93.09
	Volatility	IS	88.73	87.42	85.82	83.31
		OOS	85.99	84.48	82.52	79.00
	Spread	IS	97.77	93.84	84.16	70.12
		OOS	94.74	91.15	81.42	65.29

Table 4: Results showing the R^2 (in percentage) of the price-impact model, sorted by stock characteristics. R^2 is measured for both in-sample (IS) and out-of-sample (OOS) tests. The top panel is based on experiments using OFIs at best level. The bottom panel is based on experiments using integrated OFIs. Volume: trading volume on the previous trading day. Volatility: volatility of one-minute returns during the previous trading day. Spread: average bid-ask spread during the previous trading day. [0%, 25%), respectively [75%, 100%], denote the subset of stocks with the lowest, respectively highest, 25% values for a given stock characteristic.

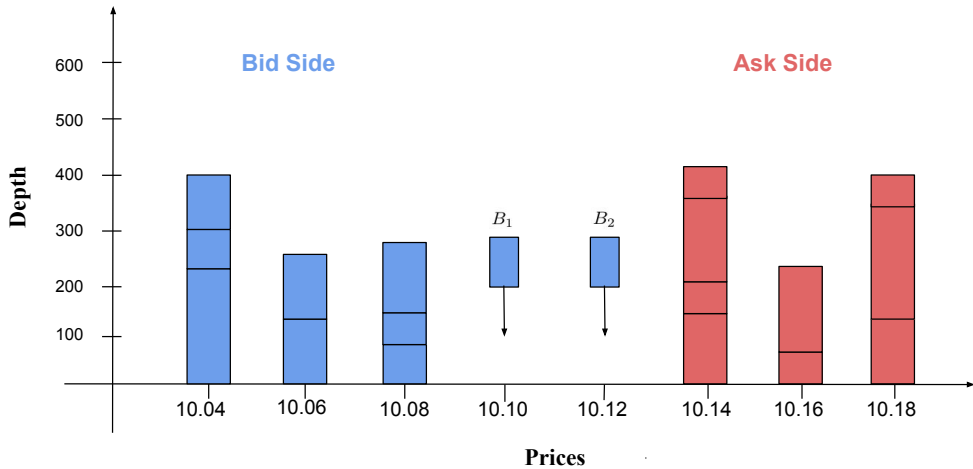


Figure 7: Two potential scenarios when a limit buy order, B_1 (B_2), arrives within the bid-ask spread with a specific target price. Assuming B_1 and B_2 have the same size but different prices, then they will lead to the same multi-level OFI vectors but different mid-prices.

4 Cross impact

In this section, we study the cross-impact model, i.e. how the stock prices are related to the order flow imbalances of other stocks. We provide a new method, applying Least Absolute Shrinkage and Selection

Operator (LASSO), to examine the existence of contemporary cross-impact.

4.1 Related literature

The cross-impact phenomenon has attracted considerable interest in the recent literature [29, 7, 11, 44, 48]. The existence of cross-impact naturally relates to problems like optimal execution of portfolios, statistical arbitrage of a set of assets, etc. If the cross-impact holds, higher execution costs occur when trading multiple assets simultaneously.

To date, most studies focus on the cross-correlation structure of returns and order flows. Hasbrouck and Seppi [29] find that commonality in returns among Dow 30 stocks is mostly attributed to order flow commonality. Wang et al. [48] empirically analyze the price responses of a given stock influenced by the trades of other stocks, which they denote as cross-response. They authors show that the average cross-responses are weaker than the self-response. Furthermore, Benzaquen et al. [7] adopt the multivariate linear propagator model to explain the facts regarding cross-response.

Other empirical studies use the multi-asset extension of the linear model proposed by Kyle [38] and investigate the off-diagonal terms, i.e. cross-impact coefficients. Pasquariello and Vega [44] provide empirical evidence of cross-asset informational effects in NYSE and NASDAQ stocks between 1993 and 2004. The authors demonstrate that the daily order flow imbalance in one stock, or across one industry, has a significant and persistent impact on daily returns of other stocks or industries.

One closely related work is Capponi and Cont [11], where the authors render a different conclusion about cross-impact from a viewpoint of causality. They first show that the positive covariance between returns of a specific stock and order flow imbalances of other stocks cannot constitute evidence of cross-impact. They decompose the order flow imbalances into a common factor and idiosyncratic components, in order to verify that, as long as the common factor is involved in the model, adding cross-impact terms improves the explained proportion of the variance only by 0.5%. Our present study differs from Capponi and Cont [11] in the following several aspects.

- (1) Capponi and Cont [11] only focus on the in-sample performance; the results in Appendix C reveal that the model proposed by them has a tendency to overfit the training data and leads to poor out-of-sample performance.
- (2) Our model takes into account the potential sparsity of the cross-impact terms, while Capponi and Cont [11] ignore this aspect; to this end, one can check more experimental results in Appendix C.
- (3) In addition to examining the cross-impact of best-level OFIs, we also consider the cross-impact from multi-level OFIs, in order to gauge a comprehensive understanding of the relations between multi-level

OFIs of different assets and individual returns. To the best of our knowledge, this is the first study to investigate such relations.

4.2 Models for Cross-impact

We use the OFIs of multiple stocks (including a stock's own OFI) as candidate features to fit the returns $r_{i,t}$ of the i -th stock, as shown in Eqn (12). In this model, $\eta_{i,t}$ is the noise term with $\mathbb{E}[\eta_{i,t}^{[1]}] = 0$ and $\text{Var}[\eta_{i,t}^{[1]}] < \infty$. Thus, $\beta_{i,j}^{[1]} (j \neq i)$ represents the influence of the j -th stock's OFI on the return of stock i , after excluding the self-impact of stock i . In addition, we also study the cross-impact model using the integrated OFIs, denoted as CI^I .

$$\text{CI}^{[1]} : r_{i,t}^{(h)} = \alpha_i^{[1]} + \beta_{i,i}^{[1]} \text{ofi}_{i,t}^{1,(h)} + \sum_{j \neq i} \beta_{i,j}^{[1]} \text{ofi}_{j,t}^{1,(h)} + \eta_{i,t}^{[1]}. \quad (12)$$

$$\text{CI}^I : r_{i,t}^{(h)} = \alpha_i^I + \beta_{i,i}^I \text{ofi}_{i,t}^{I,(h)} + \sum_{j \neq i} \beta_{i,j}^I \text{ofi}_{j,t}^{I,(h)} + \eta_{i,t}^I. \quad (13)$$

Sparsity of Cross-impact. On one hand, ordinary least squares (OLS) regression becomes ill-posed when there are fewer observations than parameters. We are considering N (the number of stocks studied in the present paper) features in Eqns (12) and (13), i.e. the contemporaneous OFIs of each stock in our universe. Assuming the studied universe consists of the components of the S&P500 index, i.e. $N \approx 500$ and the time interval is one minute, then each linear regression requires at least 500 observations, accounting for 500 minutes of historical data, i.e., more than one trading day. Therefore, it seems inappropriate to estimate Eqns (12) and (13) for intraday scenarios using OLS regression. On the other hand, Capponi and Cont [11] find that a certain number of cross-impact coefficients $\beta_{i,j} (j \neq i)$ from their OLS regressions² are not statistically significant at the 1% significance level.

Therefore, our approach assumes that there is a small number of assets $j \neq i$ having significant cross-impact on stock i , as opposed to the entire universe. To this end, we apply the Least Absolute Shrinkage and Selection Operator (LASSO) to solve Eqns (12) and (13). Note that even though the sparsity of the cross-impact terms is not theoretically guaranteed, our empirical evidences confirm this modeling assumption.

LASSO is a regression method that performs both variable selection and regularization, in order to enhance the prediction accuracy and interpretability of regression models (see more in Hastie et al. [30]). It can be formulated as linear regression models. Take Eqn (12) as an example, the objective function of LASSO consists of two parts, i.e. the sum of squared residuals, and the l_1 constraint on the regression coefficients, as shown in (14).

²The reason why Capponi and Cont [11] are able to adopt OLS regressions is that they use an entire trading day to estimate cross-impact on the basis of 67 stocks.

$$\min_{\alpha_i^{[1]}, \beta_{i,j}^{[1]}, j=1, \dots, N} \mathcal{L}_i = \sum_t \left[r_{i,t} - \alpha_i^{[1]} - \beta_{i,i}^{[1]} \text{off}^1_{i,t} - \sum_{j \neq i} \beta_{i,j}^{[1]} \text{off}^{1,(h)}_{j,t} \right]^2 + \lambda \sum_{j=1}^N \left\| \beta_{i,j}^{[1]} \right\|_1. \quad (14)$$

There is a hyperparameter λ in the loss function that controls the penalty weight. In practice, we use cross-validation [46], a standard procedure in machine learning for choosing the penalty weight for each regression. Several techniques [23, 19] from convex analysis and optimization theory have been developed to compute the solutions of LASSO, including coordinate descent, subgradient methods, least-angle regression (LARS), and proximal gradient methods. In this work, we use the coordinate descent algorithm to estimate the model.

4.3 Empirical results

Implementation. We follow the same setting as in Section 3.3 to implement the cross-impact model, and compare its in-sample and out-of-sample performance with the price-impact model. Table 5 reports the average R^2 values of the PI and CI models with normalized OFIs at the best level (in the top panel), and the results with the integrated OFIs (in the bottom panel). We observe improvements for in-sample (2.71%) and out-of-sample tests (1.39%) when using the OFIs at the best level. For integrated OFIs, the improvement for in-sample tests is 0.71%, statistically significant. However, there is no increase in out-of-sample R^2 when using the integrated OFIs. We refer the reader to Appendix B for more experimental results of cross-impact models with multi-level OFIs, which further support our observations.

		PI (%)	CI (%)	ΔR^2 (%)	p -Value
off ¹	In-Sample	71.16	73.87	2.71	0.00
	Out-Of-Sample	64.64	66.03	1.39	0.00
off ^I	In-Sample	87.14	87.85	0.71	0.00
	Out-Of-Sample	83.83	83.62	-0.21	1.00

Table 5: Average statistics of the models $\text{PI}^{[1]}$ (Eqn (6)), $\text{CI}^{[1]}$ (Eqn (12)), PI^I (Eqn (11)) and CI^I (Eqn (13)), for the **contemporaneous** returns. The first and second column report the adjusted- R^2 of the price-impact and cross-impact models, respectively. ΔR^2 is the increase in adjusted- R^2 . p -Value represents the probability of observing the increase in adjusted- R^2 under the null hypothesis of no increase. Note the results of $\text{PI}^{[1]}$ (PI^I) model in the first column are the same as those in Table 1 (Table 3), respectively.

Sparsity of the Cross-impact coefficients. Figure 8 reveals that the average number of statistically significant cross-impact coefficients ($\beta_{i,j}^{[1]} \neq 0$, when $j \neq i$) for each stock is around 10, supporting the sparsity assumption. Returns of Facebook (FB) are influenced by the smallest number (fewer than 5) of multi-asset

OFIs, while almost 27 other stocks' OFIs can affect the price movements of General Electric (GE).

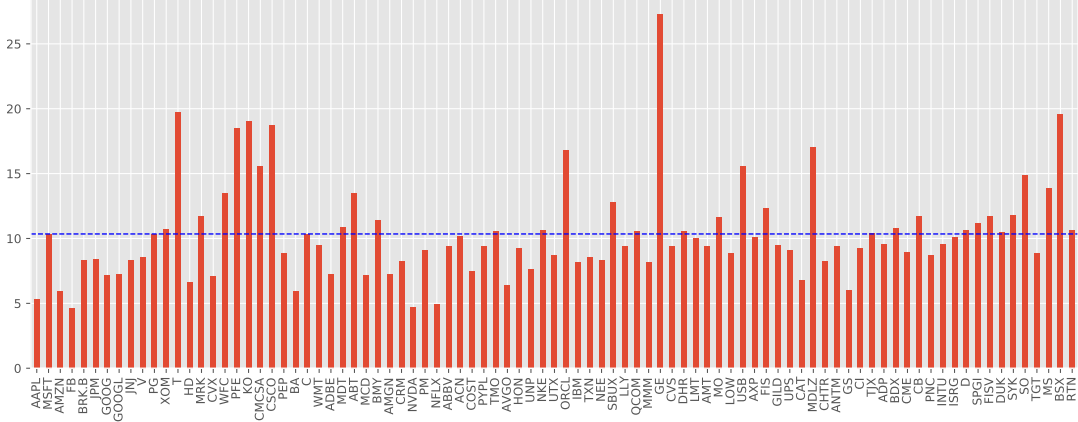


Figure 8: Bar plot showing the number of non-zero cross-impact coefficients for individual stocks averaged across days; the dashed blue line represents the average number across assets in our universe. Stocks are sorted according to their market capitalization at the end of 2019.

Next, we take a closer look at the cross-impact coefficients of each stock based on the best-level OFIs, i.e. $\beta_{i,j}^{[1]} (j \neq i)$. Figure 9 shows a comparison of the top 20 singular values of the coefficient matrices given by the best-level and integrated OFIs. The relatively large singular values of the best-level OFI is a consequence of the higher edge density and thus average degree of the network. Note that both networks exhibit a large top singular value of the adjacency matrix (akin to the usual *market mode* [39]), and the integrated OFI network has a faster decay of the spectrum, thus revealing its low rank structure.

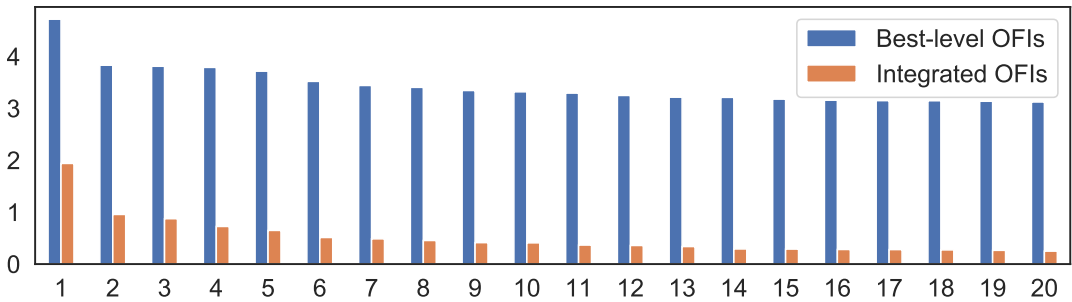


Figure 9: Barplot of singular values in descending order for the average coefficient matrix in **contemporaneous cross-impact** models. The coefficients are averaged over 2017–2019. We perform Singular Value Decomposition (SVD) on the coefficient matrix to obtain the singular values. The *x*-axis represents the singular value rank, and the *y*-axis represents the singular values.

We construct a network for each coefficient matrix, which only preserves the edges larger than the a

given threshold [36, 18], as shown in Figure 10. We color stocks according to the GICS sector division³, and sort them by their market capitalization within each sector. As one can see from Figure 10(a), the cross-impact coefficient matrix $[\beta_{i,j}^{[1]}]_{j \neq i}$ displays a sectorial structure, in accordance with previous studies (e.g. Benzaquen et al. [7]). This demonstrates that the price of a specific stock is more influenced by the OFIs of stocks in the same sector, as expected. This behaviour could be fueled by index arbitrage strategies, where traders may, for example, trade an entire basket of stocks coming from the same sector against an index.

Figure 10(b) presents the average cross-impact coefficients based on integrated OFIs, i.e. $\beta_{i,j}^I (j \neq i)$. Comparing with Figure 10(a), the connections in Figure 10(b) are much weaker, implying that the cross-impact from stocks can be potentially explained by a stock's own multi-level OFIs, to a large extent. Note that there is only one connection from GOOGL to GOOG, as pointed out at the top of Figure 10(b). This stems from the fact that both stock ticker symbols pertain to Alphabet (Google), therefore there exists a strong relation between them. Our study also revealed that OFIs of GOOGL have more influence on the returns of GOOG, not the other way around. The main reason might be that GOOGL shares have voting rights, while GOOG shares do not.

In Figures 10(c) and 10(d), we set lower threshold values (75-th / 25-th percentile of coefficients) in order to promote more edges in the networks based on integrated OFIs. More interestingly, we observed 4 connections in Figure 10(c). Except from bidirectional links between GOOGL and GOOG, there exists a one-way link from Cigna (CI) to Anthem (ANTM), and one-way link from Duke Energy (DUK) to NextEra Energy (NEE). Anthem announced to acquire Cigna in 2015. After a prolonged breakup, this merger finally failed in 2020. Therefore, it is unsurprising that the OFIs of Cigna can affect the price movements of Anthem. In terms of the second pair, NextEra was interested in acquiring Duke Energy, but Duke rebuffed the takeover in 2020. Note that 2020 is not in our sample period. This indicates that some participants in the market may have noticed the special relationship between Duke Energy and NextEra Energy before this mega-merger was proposed.

Discussion about Cross-impact. We consider the following scenario, also depicted in Figure 11, to explain the above findings. For simplicity, we denote the order from trading strategy A on stock i (resp. j) as A_i (resp. A_j). Analogously, we define orders from strategy B and S . Let us next consider the OFIs of stock i . There are three orders from different portfolios, given by A_i , B_i and S_i . A_i is at the third bid level of stock i and linked to an order at the best ask level of stock j , i.e. A_j . Also, B_i is at the best ask level of stock i and linked to an order at the best bid level of stock j , i.e. B_j . Finally, S_i is an individual bid order

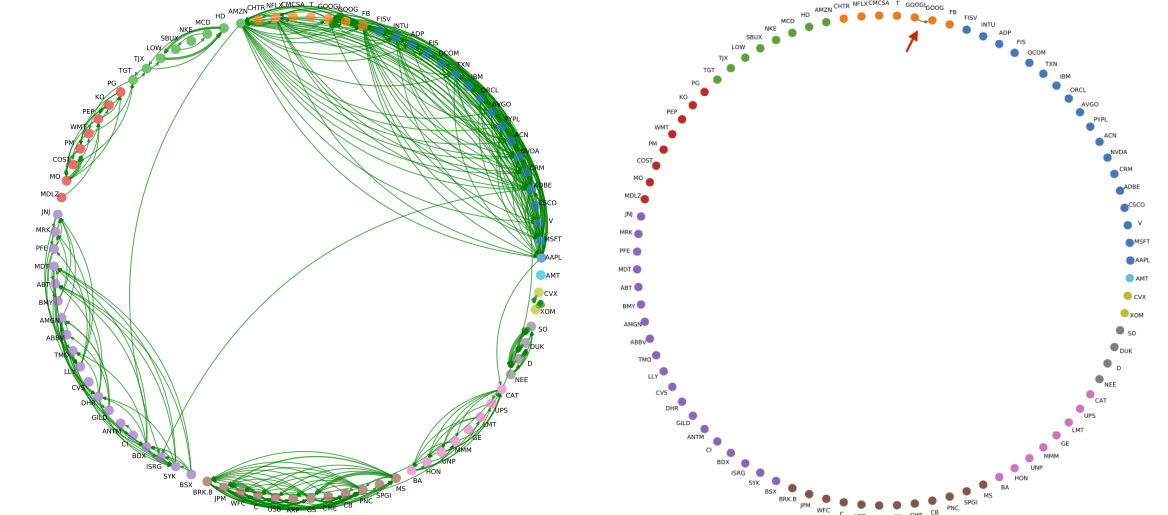
³The Global Industry Classification Standard (GICS) is an industry taxonomy developed in 1999 by MSCI and Standard & Poor's (S&P) for use by the global financial community.

at the best level of stock i .

Now assume that the best-level limit orders from stock j are linked to price movements of stock i through paths $B_j \rightarrow B_i \rightarrow \text{ofi}_i^1 \rightarrow r_i$ and $A_j \rightarrow A_i \rightarrow \text{ofi}_i^3 \rightarrow r_i$. Thus the price-impact model which only utilizes its own best-level orders of stock i will ignore the information along the second path $A_j \rightarrow A_i \rightarrow \text{ofi}_i^3 \rightarrow r_i$. This might illustrate why the best-level OFIs of multiple assets can provide additional explanatory power to the price-impact model using only the best-level OFIs.

Nonetheless, if we can integrate multi-level OFIs in an efficient way (in our example, aggregate order imbalances caused by orders A_i , B_i and S_i), then there is no need to consider OFIs from other stocks for modeling price dynamics. In other words, information hidden in the path $A_j \rightarrow A_i \rightarrow \text{ofi}_i^3 \rightarrow r_i$ can be leveraged as long as A_i is well absorbed into new integrated OFIs. We put forward this mechanism which potentially explains why the cross-impact model with integrated OFIs cannot provide extra explanatory power compared to the price-impact model with integrated OFIs, which also highlights the advantage of our integrated OFIs.

Another possible explanation for this is that the duration of the cross-impact terms might be shorter than the current time interval (30 minutes) used in our experiments, rendering the cross-impact terms to disappear in out-of-sample tests. To verify this assertion, we implement additional experiments where models are updated more frequently. The results (deferred to Appendix A) reveal that even under higher-frequency updates of the models, there is no benefit from introducing cross-impact terms to the price-impact model with integrated OFIs.



(a) Threshold = 95-th percentile, based on best-level OFIs (b) Threshold = 95-th percentile, based on integrated OFIs

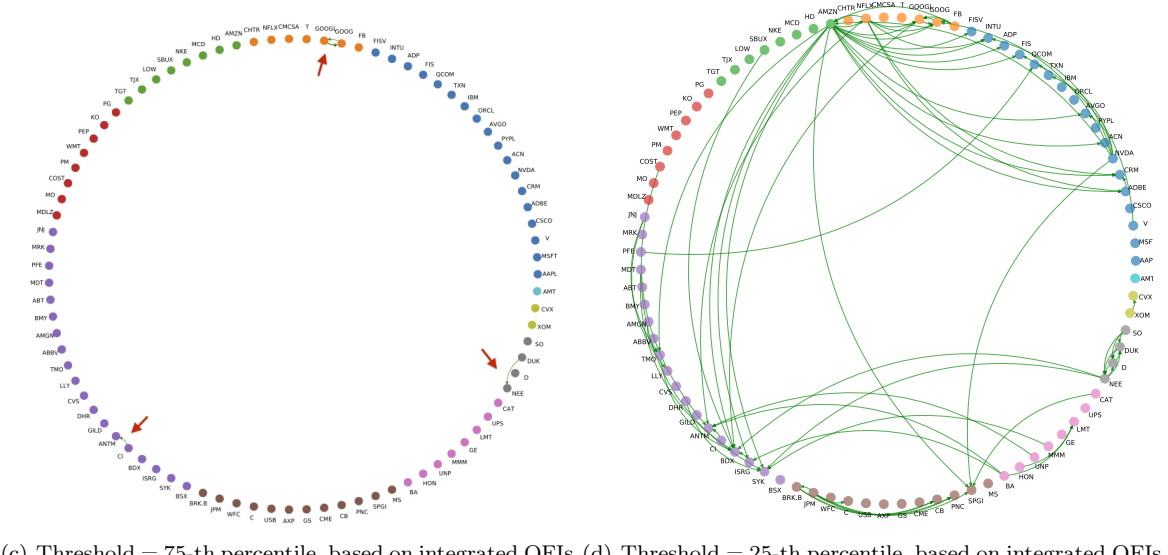


Figure 10: Illustrations of the coefficient networks constructed from **contemporaneous cross-impact** models. The coefficients are averaged over 2017–2019. To render the networks more interpretable and for ease of visualization, we only plot the top 5% largest (a-b), or top 25% largest (c), or top 75% largest (d), in magnitude coefficients. Nodes are coloured by the GICS structure and sorted by market capitalization. Green links represent positive values while black links represent negative values. The width of edges is proportional to the absolute values of their respective coefficients.

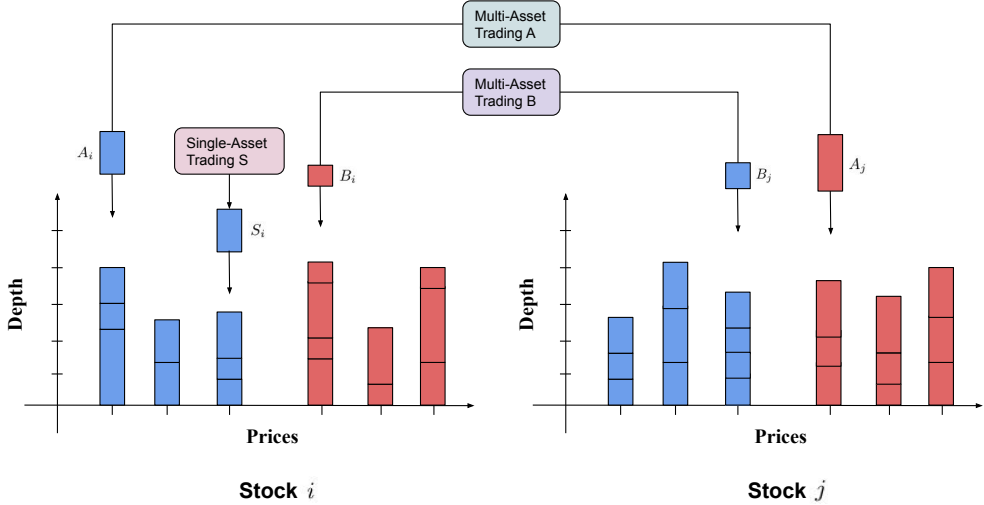


Figure 11: Illustration of the cross-impact model. The orders at different levels of each stock may come from single-asset and multi-asset trading strategies. The returns of stock i are potentially influenced by orders of stock j through the connections $B_j \rightarrow B_i \rightarrow \text{ofi}_i^1 \rightarrow r_i$ and $A_j \rightarrow A_i \rightarrow \text{ofi}_i^3 \rightarrow r_i$. Information along the path $A_j \rightarrow A_i \rightarrow \text{ofi}_i^3 \rightarrow r_i$ can be collected by the price-impact model with integrated OFIs but not by the price-impact model with only best-level OFIs.

5 Forecasting future returns

In previous sections, the definitions of price-impact and cross-impact are based on contemporaneous OFIs and returns, meaning that both quantities pertain to the same bucket of time. In this section, we extend the above studies to future returns, and probe into the forward-looking price-impact and cross-impact models.

5.1 Related literature

There is a large body of literature researching the lead-lag effect in equity returns [31, 13, 45, 42, 6] and crypto returns [3]. Hou [31] shows that within the same industry, returns of large firms help predict returns of small firms. Chinco et al. [13] apply LASSO to produce rolling one-minute-ahead return forecasts using the entire cross-section lagged returns as candidate predictors, and observe that cross-asset returns can improve Sharpe Ratios for a given trading strategy. Rapach et al. [45] investigate the role of the United States in international markets, and show that lagged U.S. returns can significantly predict returns in numerous non-U.S. industrialized countries. Menzly and Ozbas [42] find that stocks that are in economically related industries can cross-predict each other's returns.

In recent years, machine learning models, including deep neural networks, have achieved substantial

developments, leading to their applications in financial markets, especially for the task of predicting stock returns. Huck [32] utilizes state-of-the-art techniques, such as random forests, to construct a portfolio over a period of 22 years, and the results demonstrate the power of machine learning models to produce profitable trading signals. Krauss et al. [37] apply a series of machine learning methods to forecast the probability of a stock to outperform the market index, and then construct long-short portfolios from the predicted one-day-ahead trading signals. Gu et al. [25] employ machine learning methods, such as LASSO, random forest, neural networks etc., to make one-month-ahead return forecasts, and demonstrate the potential of machine learning approaches in empirical asset pricing, due to their ability to handle nonlinear interactions.

A few studies have begun to examine the relation between order imbalances and future daily returns [14, 15, 10]. Chordia et al. [14] reveal that daily stock market returns are strongly related to contemporaneous and lagged order imbalances. Chordia and Subrahmanyam [15] further find that there exists a positive relation between lagged order imbalances and daily individual stock returns. The authors also show that imbalance-based trading strategies, i.e. buy if the previous day’s imbalance is positive, and sell if the previous day’s imbalance is negative, are able to yield statistically significant profits. Cao et al. [10] show that the order imbalances behind the best level are informative, and have additional power in forecasting future short-term returns. Nonetheless, to the best of our knowledge, multi-asset order flow imbalances have not been considered as predictors for predicting future returns in the literature, which is a direction we explore in the remainder of this section.

5.2 Predictive models

We propose the following forward-looking price-impact and cross-impact models, denoted as F-PI^[1] and F-CI^[1], respectively. F-PI^[1] uses the lagged OFIs of stock i to predict its own future return $R_{i,t+1}$ ⁴, while F-CI^[1] involves the entire lagged multi-asset OFIs.

$$\text{F-PI}^{[1]} : R_{i,t+1}^{(h)} = \alpha_i^F + \beta_i^F \text{ofi}_{i,t}^{1,(h)} + \gamma_i^F \text{ofi}_{i,t-1}^{1,(h)} + \theta_i^F \text{ofi}_{i,t-2}^{1,(h)} + \epsilon_{i,t}^F. \quad (15)$$

$$\text{F-CI}^{[1]} : R_{i,t+1}^{(h)} = \alpha_i^F + \sum_{j=1}^N \left[\beta_{i,j}^F \text{ofi}_{j,t}^{1,(h)} + \gamma_{i,j}^F \text{ofi}_{j,t-1}^{1,(h)} + \theta_{i,j}^F \text{ofi}_{j,t-2}^{1,(h)} \right] + \eta_{i,t}^F. \quad (16)$$

We also study models with integrated OFIs, as shown here in Eqns (17) and (18), and denote them as F-PI ^{I} and F-CI ^{I} , respectively.

$$\text{F-PI}^I : R_{i,t+1}^{(h)} = \alpha_i^{FI} + \beta_i^{FI} \text{ofi}_{i,t}^{I,(h)} + \gamma_i^{FI} \text{ofi}_{i,t-1}^{I,(h)} + \theta_i^{FI} \text{ofi}_{i,t-2}^{I,(h)} + \epsilon_{i,t}^{FI}. \quad (17)$$

⁴For ease of interpretation in the following strategy profitability analysis, here we only report the results for forecasting the raw log-returns. In an unreported experiment, we predict the future returns normalized by volatility. We also find significant improvements in out-of-sample R^2 by introducing cross-asset terms.

$$\text{F-CI}^I : \quad R_{i,t+1}^{(h)} = \alpha_i^{FI} + \sum_{j=1}^N \left[\beta_{i,j}^{FI} \text{ofi}_{j,t}^{I,(h)} + \gamma_{i,j}^{FI} \text{ofi}_{j,t-1}^{I,(h)} + \theta_{i,j}^{FI} \text{ofi}_{j,t-2}^{I,(h)} \right] + \eta_{i,t}^{FI}. \quad (18)$$

Furthermore, we compare OFI-based models with those return-based models proposed in previous works (see Chinco et al. [13]), where the lagged returns are involved as predictors. F-AR is an autoregressive (AR) model of order 3, as shown in (19). F-CR uses the entire cross-section lagged returns as candidate predictors, as detailed in (20).

$$\text{F-AR} : \quad R_{i,t+1}^{(h)} = \alpha_i^R + \beta_i^R R_{i,t}^{(h)} + \gamma_i^R R_{i,t-1}^{(h)} + \theta_i^R R_{i,t-2}^{(h)} + \epsilon_{i,t}^R. \quad (19)$$

$$\text{F-CR} : \quad R_{i,t+1}^{(h)} = \alpha_i^R + \sum_{j=1}^N \left[\beta_{i,j}^R R_{j,t}^{(h)} + \gamma_{i,j}^R R_{j,t-1}^{(h)} + \theta_{i,j}^R R_{j,t-2}^{(h)} \right] + \eta_{i,t}^R. \quad (20)$$

5.3 Empirical results

Implementation. In this experiment, observations associated with returns and OFIs are computed minutely, i.e. $h = 1$ minute. We use data from the previous 30 minutes to estimate the model parameters and apply the fitted model to forecast the one-minute-ahead return. We repeat this procedure for each trading day, to compute *rolling one-minute-ahead return forecasts*.

		F-PI (%)	F-CI (%)	ΔR^2 (%)	<i>p</i> -Value
ofi ¹	In-Sample	0.24	12.24	12.00	0.00
	Out-Of-Sample	-19.07	-11.98	7.09	0.00
ofi ^I	In-Sample	0.26	12.19	11.93	0.00
	Out-Of-Sample	-17.62	-11.81	5.81	0.00
		F-AR (%)	F-CR (%)	ΔR^2 (%)	<i>p</i> -Value
<i>R</i>	In-Sample	0.38	13.66	13.28	0.00
	Out-Of-Sample	-36.62	-11.19	25.43	0.16

Table 6: Statistics of models using lagged OFIs (in the top panel), including F-PI^[1] (Eqn (15)), F-CI^[1] (Eqn (16)), along with their integrated OFI-based counterparts denoted as F-PI^{*I*} (Eqn (17)) and F-CI^{*I*} (Eqn (18)), and models using lagged returns (in the bottom panel), including F-AR (Eqn (19)) and F-CR (Eqn (20)), for predicting **future** returns. The first and second column report the adjusted- R^2 of price-impact and cross-impact model, respectively. ΔR^2 is the increase in adjusted- R^2 . *p*-Value represents the probability of observing the increase in adjusted- R^2 under the null hypothesis of no increase.

Table 6 summarizes the in-sample and out-of-sample performance of the aforementioned predictive models. It is not surprising that the cross-impact models F-CI^[1] (resp. F-CI^{*I*}) attain higher adjusted- R^2 statistics compared to the price-impact models F-PI^[1] (resp. F-PI^{*I*}), for the in-sample tests. In terms of out-of-sample R^2 performance, F-CI^[1] and F-CI^{*I*} show an improvement of 7.09% and 5.81%, respectively. For models using

lagged returns, we reach a similar conclusion as in Chinco et al. [13], that lagged cross-asset returns can improve both in-sample and out-of-sample R^2 .

We remark that negative R^2 values do not imply that the forecasts are economically meaningless. To emphasize this point, we will incorporate these return forecasts into two common forecast-based trading strategies, and showcase their profitability in the following subsection.

Coefficient network. Considering the different magnitudes of the OFIs and returns, we first normalize the coefficient matrix of each model by dividing by the average of the absolute coefficients. We construct a network for each normalized coefficient matrix, which only preserves the edges larger than the 95-th percentile of coefficients. Figure 12 illustrates some of the main characteristics of the coefficient networks for various forward-looking models, including F-CI^[1] (Eqn (16)), F-CI^I (Eqn (18)), F-CR (Eqn (20)).

To gain a better understanding of the structural properties of the resulting network, we aggregate node centrality measures [21] at the sector level, and also perform a spectral analysis of the adjacency matrix [35, 43]. From Table 8, we observe that on average, the network based on best-level OFIs contains more inner-sector connections than the other two counterparts, thus implying a sectorial structure. Table 7 presents the top five most significant stocks in terms of out-degree centrality in each network. For example, in Figure 12(a), Amazon (AMZN), Google (GOOGL, GOOG), Nvidia (NVDA), NFLX (Netflix) are five hubs that possess the highest predictive power for other stocks, thus hinting at the possibility of building cross-asset models. Interestingly, Figure 12(b) shows that even though Amazon, Netflix and Nvidia are still hubs, Google is replaced by Goldman Sachs (GS) and Facebook (FB). In Figure 12(c), Intuitive Surgical (ISRG), Broadcom (AVGO) and General Electric (GE) are new hubs, while Amazon (AMZN) is not.

Figure 13 shows a barplot with the average value for the top 20 largest singular values of the network adjacency matrix, for best-level OFIs, integrated OFI, and returns, where the average is performed over all constructed networks. For ease of visualization and comparison, we first normalize the adjacency matrix before computing the top singular values, which exhibit a fast decay. In addition to the significantly large top singular value revealing that the networks have a strong rank-1 structure, the next 6-8 singular values are likely to correspond to the more prominent industry sectors.

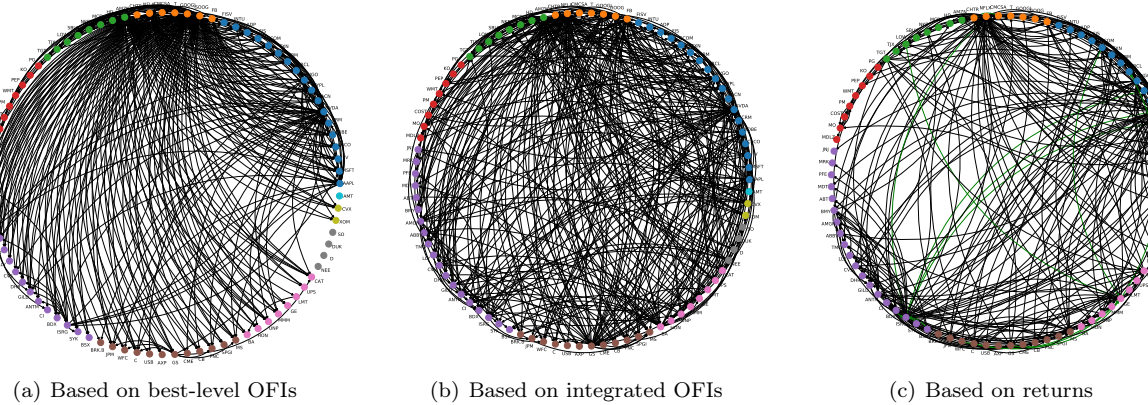


Figure 12: Network structure of the coefficient matrix constructed from **forward-looking cross-impact** models. The coefficients are averaged over 2017–2019. To render the networks more interpretable and for ease of visualization, we only plot the top 5% largest in magnitude coefficients. Nodes are coloured by the GICS structure and sorted by market capitalization. Green links represent positive values while black links represent negative values. The width of edges is proportional to the absolute values of their respective coefficients.

Best-level OFIs	Integrated OFIs	Returns
AMZN	NFLX	NVDA
GOOG	AMZN	NFLX
GOOGL	NVDA	ISRG
NVDA	GS	AVGO
NFLX	FB	GE

Table 7: Top 5 stocks according to node out-degree centrality in threshold networks shown in Figure 12. The out-degree centrality for a specific node is the fraction of nodes its outgoing edges are connected to.

	Group In-degree Centrality			Group Out-degree Centrality		
	Best-level OFIs	Integrated OFIs	Returns	Best-level OFIs	Integrated OFIs	Returns
Information Technology	0.12	0.36	0.26	0.46	0.62	0.59
Communication Services	0.06	0.24	0.20	0.85	0.74	0.60
Consumer Discretionary	0.09	0.20	0.15	0.86	0.51	0.17
Consumer Staples	0.03	0.15	0.09	0.00	0.11	0.01
Health Care	0.10	0.37	0.19	0.12	0.22	0.59
Financials	0.12	0.21	0.17	0.03	0.41	0.08
Industrials	0.10	0.19	0.20	0.00	0.39	0.27
Utilities	0.00	0.07	0.04	0.00	0.06	0.00
Energy	0.06	0.07	0.04	0.00	0.14	0.00
Real Estate	0.00	0.05	0.02	0.00	0.00	0.01

Table 8: Group degree centrality for each GICS sector. According to the threshold networks as shown in Figure 12, we compute the the fraction of stocks outside of a specific sector connected to stocks in this specific sector. The color of each sector in this table corresponds to the color in Figure 12.

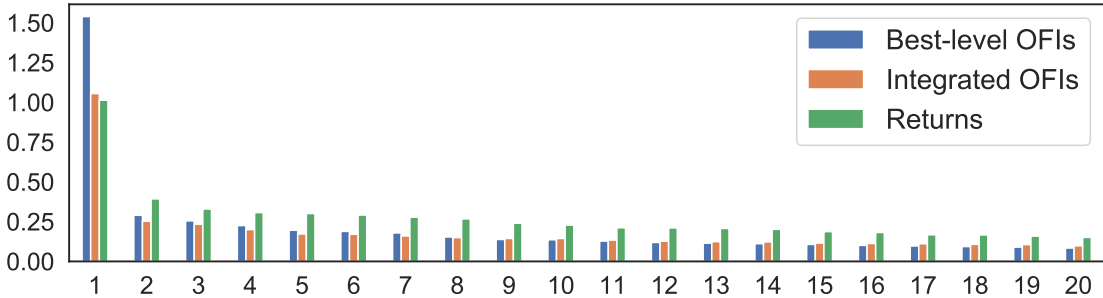


Figure 13: Barplot of normalized singular values in descending order for the average coefficient matrix in **forward-looking cross-impact** models. The coefficients are averaged over 2017–2019. We perform Singular Value Decomposition (SVD) on the coefficient matrix and obtain the singular values. The x -axis represents the singular value rank, and the y -axis shows the normalized singular values.

5.4 Strategy Profitability Analysis

On the basis of one-minute-ahead return forecasts, we employ two common portfolio construction methods to evaluate the economic gains of the aforementioned predictive models.

Forecast-implied portfolio. Chinco et al. [13] propose a method for portfolio construction based on predicted returns from a specific forecasting model F , denoted as forecast-implied portfolio. The motivations can be summarized as follows.

- It only executes an order when the one-minute-ahead return forecast exceeds the bid-ask spread.
- It buys/sells more shares of the i -th stock when the absolute value of one-minute-ahead return forecast for i -th stock is higher.
- It buys/sells more shares of the i -th stock when the one-minute-ahead return forecasts for the i -th stock tend to be less volatile throughout the trading day.

This strategy allocates a fraction $w_{i,t}$ of its capital to the i -th stock, based on

$$w_{i,t} \stackrel{\text{def}}{=} \frac{1_{\{|f_{i,t}^F| > sprd_{i,t}\}} \cdot f_{i,t}^F / \sigma_{i,t}^F}{\sum_{n=1}^N 1_{\{|f_{n,t}^F| > sprd_{n,t}\}} \cdot |f_{n,t}^F| / \sigma_{n,t}^F}. \quad (21)$$

Here $f_{i,t}^F$ represents the one-minute-ahead return forecast according to model F for minute $(t+1)$, $sprd_{i,t}$ represents the relative bid-ask spread at time t , $\sigma_{i,t}^F$ represents the standard deviation of the model's one-minute-ahead return forecasts for the i -th stock during the previous 30 minutes of trading, i.e. the standard

deviation of in-sample fits. The denominator is the total investment, so that the strategy is self-financed. If there are no stocks with forecasts that exceed the spread in a given minute, then we set $w_{i,t} = 0, \forall i$.

Long-short portfolio. In this strategy, we sort stocks into deciles according to forecast returns of model F . We then construct a portfolio that longs stocks with the highest forecast return (in decile 10), and shorts stocks with the lowest ones (in decile 1). We refer to this portfolio as the long-short portfolio [37]. Its weights are calculated as follows

$$w_{i,t} \stackrel{\text{def}}{=} \frac{1_{\{f_{i,t}^F > d_t^{(9)}\}} - 1_{\{f_{i,t}^F < d_t^{(1)}\}}}{\sum_{n=1}^N \left[1_{\{f_{n,t}^F > d_t^{(9)}\}} + 1_{\{f_{n,t}^F < d_t^{(1)}\}} \right]}. \quad (22)$$

Here $f_{i,t}^F$ is the one-minute-ahead return forecast according to model F for minute $(t+1)$. $d_t^{(1)}$ and $d_t^{(9)}$ represent the lowest and highest one tenth predicted returns of stocks, respectively. Alternatively, $d_t^{(1)} = \inf\{x \in \mathbb{R} : \frac{1}{N} \sum_{n=1}^N 1_{\{f_{n,t}^F \leq x\}} \geq 10\%\}$ and $d_t^{(9)} = \inf\{x \in \mathbb{R} : \frac{1}{N} \sum_{n=1}^N 1_{\{f_{n,t}^F \leq x\}} \geq 90\%\}$. The denominator is used to normalize the weights, so that the sum of the absolute weights equals 1.

Finally, we compute the *profit and loss* (PnL) of the resulting portfolios at each minute. Recall that $R_{i,t}$ is the raw log return of stock i at time t , thus $(e^{R_{i,t}} - 1)$ is the raw return.

$$\text{PnL}_{t+1}^F = \sum_{i=1}^N w_{i,t} \times (e^{R_{i,t+1}} - 1). \quad (23)$$

Performance. Table 9 compares the performance of the above two strategies, based on forecast returns from various predictive models. It is worth noting that in the following analysis, the strategy **ignores trading costs**, as this is not the focus of our paper; furthermore, we report the PnL in basis points, for ease of comparison with typical transaction fees, often also reported in basis points. Table 9 reveals that portfolios based on forecasts of the forward-looking cross-impact model outperform those based on forecasts of the forward-looking price-impact model. We also note that compared with models using the lagged returns as predictors, the models incorporating lagged OFIs yield higher PnL, implying that the OFIs contain more predictive information than the returns. We deem this to be an interesting finding, and are not aware of previous works in the literature that provided empirical evidence in this direction.

The results in Table 10 indicate that the profitability of F-CI is relatively stable during 2017-2019, but F-PI experienced a steep fall in the last quarter of 2017. Future research should be undertaken to investigate this phenomenon, preferably over a more extended period of time.

PnL (bps)	Forecast-implied	Long-short
F-PI ^[1]	0.19	0.10
F-CI ^[1]	0.99	0.91
F-PI ^I	0.20	0.12
F-CI ^I	0.92	0.86
F-AR	-0.14	-0.29
F-CR	0.88	0.58

Table 9: Results of the PnLs of two trading strategies based on different **forward-looking** models. The top, middle and bottom panels report results of models using lagged best-level OFIs (F-PI^[1], F-CI^[1]), lagged integrated OFIs (F-PI^I, F-CI^I), and lagged returns (F-AR, F-CR), respectively.

	2017				2018				2019				
	Q1	Q2	Q3	Q4	Q1	Q2	Q3	Q4	Q1	Q2	Q3	Q4	
OOS R^2 (%)	F-PI ^[1]	-17.59	-16.85	-17.27	-17.01	-17.08	-17.1	-17.83	-17.92	-15.9	-17.86	-18.91	-18.23
	F-CI ^[1]	-11.33	-11.35	-11.11	-10.84	-11.79	-11.47	-11.82	-13.08	-10.43	-12.18	-12.75	-12.10
PnL (bps)	F-PI ^[1]	0.21	0.18	0.23	-0.59	-0.08	0.30	0.38	0.44	0.30	0.21	0.25	0.46
	F-CI ^[1]	0.84	0.79	0.95	0.89	1.08	1.08	1.03	1.23	1.02	1.08	1.07	0.87

Table 10: Average statistics of the forward-looking models F-PI^[1] (Eqn (15)), and F-CI^[1] (Eqn (16)). Q1, respectively Q4, denote the first, respectively last, quarter in a year. OOS R^2 is the out-of-sample R^2 . PnL is average PnL in each minute for each quarter.

Discussion on the forward-looking models. Tables 5 and 6 reveal that, in contrast to the price-impact model, multi-asset OFIs can provide considerably more additional explanatory power for *future returns* compared to *contemporaneous returns*. A possible explanation for this asymmetric phenomenon is that there exists a time lag between when the OFIs of a given stock are formed (a so-called *flow formation period*) and the actual time when traders notice this change of flow and incorporate it into their trading models. For example, assume a trader submitted an unexpectedly large amount of buy limit orders of Apple (AAPL) at 10:00, at either the first level or potentially deeper in the book. Other traders (most likely, not high-frequency players) may notice this anomaly and adjust their portfolios (including Apple) at a much later time, for example 10:01. In this case, the OFIs of Apple may indicate future price changes of other stocks.

Consistent with our explanation, Hou [31] argues that the gradual diffusion of industry information is a leading cause of the lead-lag effect in stock returns. Cohen and Frazzini [16] find that certain stock prices do not promptly incorporate news pertaining to economically related firms, due to the presence of investors subject to attention constraints. Further research should be undertaken to investigate the origins of success of multi-asset OFIs in predicting future returns.

It is also interesting to note that forward-looking models using integrated OFIs (the bottom panel in

Table 6) cannot significantly outperform models using the best-level OFIs (the top panel in Table 6). This phenomenon might stem from the fact that the integrated OFIs do not explicitly take into account the level information (distance of a given level to the best bid/ask) of multi-level OFIs, and are agnostic to different sizes resting at different levels on the bid and ask sides of the book. To verify this claim, we conduct experiments of forward-looking price-impact models with multi-level OFIs in Appendix D. The results support our earlier intuition that certain level-specific information, useful for predicting future returns, is lost in the integration process of the multi-level OFIs. In accordance with our findings, previous studies (such as Hasbrouck and Saar [28], Cao et al. [10]) have demonstrated that limit orders at different price levels may contain different information content with respect to predicting future returns.

5.5 Price-impact at multiple future return horizons

The remainder of this Section 5 is devoted to the study of price impact of the best-level OFI on the future price returns, at multiple time horizons. The motivation for this analysis stems from the importance of the order flow for optimal execution services and market making amongst practitioners. To this end, we provide the following two approaches. To facilitate notation in this section, we ignore the subscript for stocks. OFIs and returns are computed minutely, i.e. fixing $h = 1$ min.

PnL-based. In this final experiment, we turn to study the profitability of a simple OFI-based trading strategy (see Chordia and Subrahmanyam [15]), i.e. to long a stock if its current OFI is positive, and short if the current OFI is negative, then hold for a specific period. We compute the profit and loss (PnL) as follows, and consider PnL_p as the daily PnL in a holding period p .

$$\begin{aligned} \text{PnL}_{t,p} &= \text{sign}(\text{ofi}_t^1) \times \sum_{l=1}^p R_{t+l} \\ \text{PnL}_p &= \frac{1}{N_p} \sum_{t < t_{\max}} \text{PnL}_{t,p}, \end{aligned} \tag{24}$$

where N_p is the number of time buckets and t_{\max} is the time of the last OFI. For example, if we study the PnLs of minutely OFIs over the next 1 hour, i.e. $p = 60$ min, then $N_p = 330$ and $t_{\max} = 15:00$. An example of the PnL calculation is depicted in Figure 14.

Figure 15 shows the PnL profile curve, as a function of the holding period. We find that the OFI over a given bucket, attains the highest PnL over the following 2-3 minutes; this PnL remains positive for up to approx 12 minutes, beyond which the PnL becomes slightly negative.

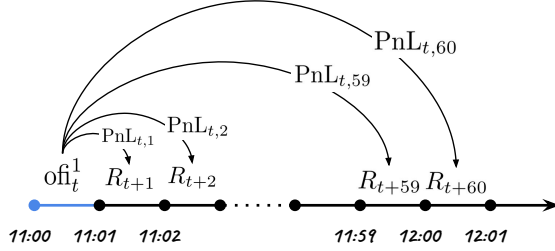


Figure 14: Illustration of PnLs over multiple horizons for a specific OFI.

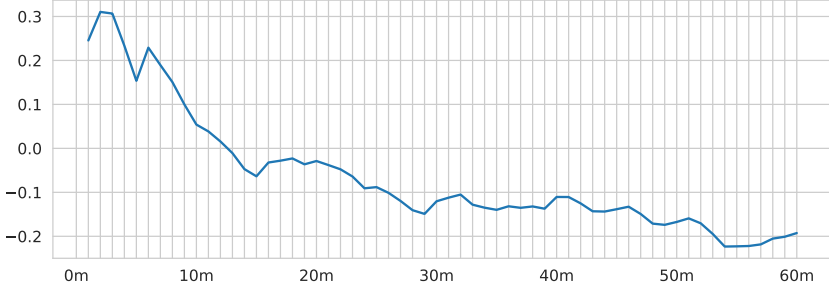


Figure 15: Average PnL as a function of the holding period; the results are averaged across stocks and days. The x -axis represents the future horizon (in minutes), while the y -axis denotes the average PnLs (in bps).

Impact-based. In this method, we first estimate the following model for each stock. In F-PI^{MF} , the coefficient β_s represents the impact of ofi_{t-s+1}^1 (i.e. OFIs in $(t-s, t-s+1]$) on R_{t+1} (i.e. return in $(t, t+1]$) after excluding the influences from other order flows during $(t-p, t]$,

$$\text{F-PI}^{MF} : \quad r_{t+1} = \alpha^{MF} + \sum_{s=1}^p \beta_s \text{ofi}_{t-s+1}^1 + \eta_t^{MF}. \quad (25)$$

Figure 16 provides an example to illustrate the connection between the model (25) and the impact of a specific ofi^1 on multi-horizon future returns. In this example, we focus on the impact of order flow imbalance in $(11:59, 12:00]$ (the blue line in each panel). At $t = 12:00$, we see that the impact of one unit of ofi^1 in $(11:59, 12:00]$ on the return in $(12:00, 12:01]$ is β_1 (the red curve in the top panel). Similarly, at $t = 12:01$, the impact of one unit of ofi^1 in $(11:59, 12:00]$ on the return in $(12:01, 12:02]$ is β_2 (the red curve in the bottom panel). Thus we conclude that the impact of a specific $\text{ofi}_{t_0}^1$ on future returns in $(t, t+1]$ ($t \geq t_0$) can be considered as β_{t+1-t_0} . Furthermore, the cumulative future price changes or returns up to time $t+1$ ($t \geq t_0$) due to $\text{ofi}_{t_0}^1$ are the cumulative sum of coefficients $\sum_{s=1}^{t+1-t_0} \beta_s$.

In order to perform a granular analysis of the multi-horizon impact, while still maintaining the computations feasible, we update the forecasting model F-PI^{MF} every day rather than every 1-min or 30-min. Figure 17 reveals that in the first bucket after the creation of a specific OFI, on average, the price is increasing

because the first coefficient is positive. However, after the first phase, the coefficients are mostly negative, implying prices are decreasing. Finally, the OFI loses its impact on price dynamics at around 55 minutes after its arrival.

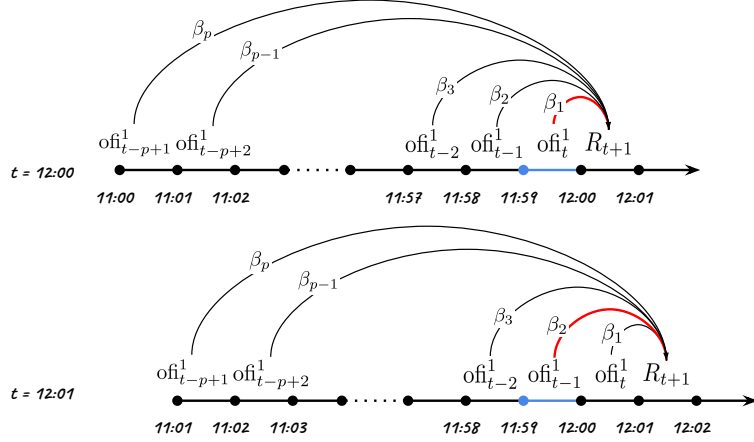


Figure 16: Illustration of price impact of a specific ofi^1 in $(11:59, 12:00]$ on the multi-horizon future returns. Coefficients $\{\beta_1, \dots, \beta_p\}$ are estimated from model (25).

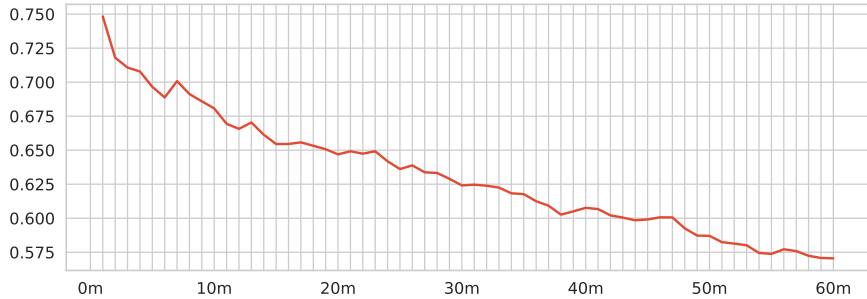


Figure 17: Cumulative sum of the coefficients in model (25). The x -axis represents the future horizons (in minutes); the y -axis represents the cumulative sum of coefficients (in basis points). Coefficients are averaged across stocks and days.

6 Conclusion

We have systematically examined the price impact of order flow imbalance from multiple perspectives. The main contributions can be summarized as follows.

First, we verify the effects of multi-level OFIs on price dynamics. We find that, as more multi-level OFIs are included as predictors, the explained percentage of total variance steadily increases in in-sample tests,

but the increments become smaller as we go deeper in the book. Meanwhile, the model’s performance in out-of-sample tests gets worse after a certain level of OFIs. This is a sign of overfitting and implies the redundancy of information in multi-level OFIs. We also observe a strong multi-collinearity across multi-level OFIs, leading us to perform principal component analysis on them. The results show that the first principal component can explain a large proportion (over 80%) of the total variance. In order to avoid overfitting, we propose to transform multi-level OFIs into an integrated variation according to the first principal component. Our integrated OFIs demonstrate a higher R^2 in spite of time-series variations and cross-sectional variations in out-of-sample tests. Interestingly, R^2 values of the price-impact model are found to be linked to bid-ask spread, volatility, and volume.

Second, we introduce a new procedure to examine the cross-impact on contemporaneous returns. Under the sparsity assumption of cross-impact coefficients, we use LASSO to describe such a structure and compare the performances with the price-impact model, which only utilizes a stock’s own OFIs. We implement models with the best-level OFIs and integrated OFIs, respectively. The results demonstrate that in comparison with the price-impact model using best-level OFIs, the cross-impact model can provide additional explanatory power, small but significant, in both in-sample and out-of-sample tests. However, the cross-impact model with integrated OFIs cannot provide extra explanatory power to the price-impact model with integrated OFIs, indicating the effectiveness of our integrated OFIs.

At last, we apply the price-impact and cross-impact models to the challenging task of predicting future returns. The results reveal that involving multi-asset OFIs can increase both in-sample and out-of-sample R^2 . We subsequently demonstrate that this increase in out-of-sample R^2 leads to additional profits, when incorporated in common trading strategies.

Future research directions. There are a number of interesting avenues to explore in future research. One such direction pertains to the assessment of whether cross-asset **multi-level** OFIs can improve the forecast of future returns (in the present work, we only considered the best-level OFI and integrated OFI). Another interesting direction pertains to performing a similar analysis as in the present paper, but for the last 15-30 minutes of the trading day, where a significant fraction of the total daily trading volume occurs. For example, according to [5], for the first few months of 2020 in the US equity market, about 23% of trading volume in the 3,000 largest stocks by market value has taken place after 3:30 p.m, compared with about 4% from 12:30 p.m. to 1 p.m. It would be an interesting study to explore the interplay between the OFI dynamics and this surge of volume at the end of US market hours.

References

- [1] Abhyankar, A., D. Ghosh, E. Levin, and R. Limmack (1997). Bid-ask spreads, trading volume and volatility: Intra-day evidence from the london stock exchange. *Journal of Business Finance & Accounting* 24(3), 343–362.
- [2] Ahn, H.-J., K.-H. Bae, and K. Chan (2001). Limit orders, depth, and volatility: Evidence from the stock exchange of hong kong. *The Journal of finance* 56(2), 767–788.
- [3] Albers, J., M. Cucuringu, S. Howison, and A. Y. Shestopaloff (2021). Fragmentation, Price Formation, and Cross-Impact in Bitcoin Markets. *arXiv 2108.09750*.
- [4] Avellaneda, M. and J.-H. Lee (2010). Statistical arbitrage in the us equities market. *Quantitative Finance* 10(7), 761–782.
- [5] Banerji, G. (2020). The 30 minutes that can make or break the trading day.
- [6] Bennett, S., M. Cucuringu, and G. Reinert (2021). Detection and clustering of lead-lag networks for multivariate time series with an application to financial markets. *7th SIGKDD Workshop on Mining and Learning from Time Series (MiLeTS)*.
- [7] Benzaquen, M., I. Mastromatteo, Z. Eisler, and J.-P. Bouchaud (2017). Dissecting cross-impact on stock markets: An empirical analysis. *Journal of Statistical Mechanics: Theory and Experiment* 2017(2), 023406.
- [8] Bouchaud, J.-P. (2010). Price impact. *Encyclopedia of quantitative finance*.
- [9] Brown, P., D. Walsh, and A. Yuen (1997). The interaction between order imbalance and stock price. *Pacific-Basin Finance Journal* 5(5), 539–557.
- [10] Cao, C., O. Hansch, and X. Wang (2009). The information content of an open limit-order book. *Journal of Futures Markets: Futures, Options, and Other Derivative Products* 29(1), 16–41.
- [11] Capponi, F. and R. Cont (2020). Multi-asset market impact and order flow commonality. *Available at SSRN*.
- [12] Chan, K. and W.-M. Fong (2000). Trade size, order imbalance, and the volatility–volume relation. *Journal of Financial Economics* 57(2), 247–273.
- [13] Chinco, A., A. D. Clark-Joseph, and M. Ye (2019). Sparse signals in the cross-section of returns. *The Journal of Finance* 74(1), 449–492.

[14] Chordia, T., R. Roll, and A. Subrahmanyam (2002). Order imbalance, liquidity, and market returns. *Journal of Financial economics* 65(1), 111–130.

[15] Chordia, T. and A. Subrahmanyam (2004). Order imbalance and individual stock returns: Theory and evidence. *Journal of Financial Economics* 72(3), 485–518.

[16] Cohen, L. and A. Frazzini (2008). Economic links and predictable returns. *The Journal of Finance* 63(4), 1977–2011.

[17] Cont, R., A. Kukanov, and S. Stoikov (2014). The price impact of order book events. *Journal of financial econometrics* 12(1), 47–88.

[18] Curme, C., M. Tumminello, R. N. Mantegna, H. E. Stanley, and D. Y. Kenett (2015). Emergence of statistically validated financial intraday lead-lag relationships. *Quantitative Finance* 15(8), 1375–1386.

[19] Efron, B., T. Hastie, I. Johnstone, and R. Tibshirani (2004). Least angle regression. *The Annals of statistics* 32(2), 407–499.

[20] Eisler, Z., J.-P. Bouchaud, and J. Kockelkoren (2012). The price impact of order book events: market orders, limit orders and cancellations. *Quantitative Finance* 12(9), 1395–1419.

[21] Everett, M. G. and S. P. Borgatti (1999). The centrality of groups and classes. *The Journal of mathematical sociology* 23(3), 181–201.

[22] Frazzini, A., R. Israel, and T. J. Moskowitz (2012). Trading costs of asset pricing anomalies. *Fama-Miller Working Paper, Chicago Booth Research Paper* (14-05).

[23] Friedman, J., T. Hastie, and R. Tibshirani (2010). Regularization paths for generalized linear models via coordinate descent. *Journal of statistical software* 33(1), 1.

[24] Giot, P. (2005). Market risk models for intraday data. *The European Journal of Finance* 11(4), 309–324.

[25] Gu, S., B. Kelly, and D. Xiu (2020). Empirical asset pricing via machine learning. *The Review of Financial Studies* 33(5), 2223–2273.

[26] Guo, X. and M. Zervos (2015). Optimal execution with multiplicative price impact. *SIAM Journal on Financial Mathematics* 6(1), 281–306.

[27] Harris, L. E. and V. Panchapagesan (2005). The information content of the limit order book: evidence from NYSE specialist trading decisions. *Journal of Financial Markets* 8(1), 25–67.

[28] Hasbrouck, J. and G. Saar (2002). Limit orders and volatility in a hybrid market: The Island ECN. *Stern School of Business Dept. of Finance Working Paper FIN-01-025*.

[29] Hasbrouck, J. and D. J. Seppi (2001). Common factors in prices, order flows, and liquidity. *Journal of financial Economics* 59(3), 383–411.

[30] Hastie, T., R. Tibshirani, and J. Friedman (2009). *The elements of statistical learning: data mining, inference, and prediction*. Springer Science & Business Media.

[31] Hou, K. (2007). Industry information diffusion and the lead-lag effect in stock returns. *The Review of Financial Studies* 20(4), 1113–1138.

[32] Huck, N. (2019). Large data sets and machine learning: Applications to statistical arbitrage. *European Journal of Operational Research* 278(1), 330–342.

[33] Jolliffe, I. T. (1986). Principal components in regression analysis. In *Principal component analysis*, pp. 129–155. Springer.

[34] Jolliffe, I. T. and J. Cadima (2016). Principal component analysis: a review and recent developments. *Philosophical Transactions of the Royal Society A: Mathematical, Physical and Engineering Sciences* 374(2065), 20150202.

[35] Kannan, R. and S. Vempala (2009). Spectral algorithms. *Foundations and Trends® in Theoretical Computer Science* 4(3–4), 157–288.

[36] Kenett, D. Y., M. Tumminello, A. Madi, G. Gur-Gershgoren, R. N. Mantegna, and E. Ben-Jacob (2010). Dominating clasp of the financial sector revealed by partial correlation analysis of the stock market. *PLoS one* 5(12), e15032.

[37] Krauss, C., X. A. Do, and N. Huck (2017). Deep neural networks, gradient-boosted trees, random forests: Statistical arbitrage on the S&P 500. *European Journal of Operational Research* 259(2), 689–702.

[38] Kyle, A. S. (1985). Continuous auctions and insider trading. *Econometrica: Journal of the Econometric Society*, 1315–1335.

[39] Laloux, L., P. Cizeau, M. Potters, and J.-P. Bouchaud (2000). Random matrix theory and financial correlations. *International Journal of Theoretical and Applied Finance* 3(03), 391–397.

[40] Lillo, F., J. D. Farmer, and R. N. Mantegna (2003). Master curve for price-impact function. *Nature* 421(6919), 129–130.

[41] Madhavan, A., M. Richardson, and M. Roomans (1997). Why do security prices change? A transaction-level analysis of NYSE stocks. *The Review of Financial Studies* 10(4), 1035–1064.

[42] Menzly, L. and O. Ozbas (2010). Market segmentation and cross-predictability of returns. *The Journal of Finance* 65(4), 1555–1580.

[43] Newman, M. Networks of information. In *Networks*. Oxford University Press.

[44] Pasquariello, P. and C. Vega (2015). Strategic cross-trading in the US stock market. *Review of Finance* 19(1), 229–282.

[45] Rapach, D. E., J. K. Strauss, and G. Zhou (2013). International stock return predictability: what is the role of the United States? *The Journal of Finance* 68(4), 1633–1662.

[46] Shao, J. (1993). Linear model selection by cross-validation. *Journal of the American statistical Association* 88(422), 486–494.

[47] Taranto, D. E., G. Bormetti, J.-P. Bouchaud, F. Lillo, and B. Tóth (2018). Linear models for the impact of order flow on prices. I. History dependent impact models. *Quantitative Finance* 18(6), 903–915.

[48] Wang, S., R. Schäfer, and T. Guhr (2016a). Average cross-responses in correlated financial markets. *The European Physical Journal B* 89(9), 207.

[49] Wang, S., R. Schäfer, and T. Guhr (2016b). Cross-response in correlated financial markets: individual stocks. *The European Physical Journal B* 89(4), 105.

[50] Wold, S., K. Esbensen, and P. Geladi (1987). Principal component analysis. *Chemometrics and intelligent laboratory systems* 2(1-3), 37–52.

[51] Wyart, M., J.-P. Bouchaud, J. Kockelkoren, M. Potters, and M. Vettorazzo (2008). Relation between bid-ask spread, impact and volatility in order-driven markets. *Quantitative finance* 8(1), 41–57.

[52] Xu, K., M. D. Gould, and S. D. Howison (2018). Multi-level order-flow imbalance in a limit order book. *Market Microstructure and Liquidity* 4(03n04), 1950011.

A High-frequency updates of contemporaneous models

In this experiment, we use a 30-minute window to estimate LASSO regressions. We then apply the estimated coefficients to fit data in the next one minute, and repeat this procedure every minute. Results are summarized in Table 11, and reveals similar conclusions as in Section 4.

		PI (%)	CI (%)	ΔR^2 (%)	<i>p</i> -Value
ofi ¹	In-Sample	70.80	73.55	2.75	0.00
	Out-Of-Sample	59.67	61.46	1.79	0.00
ofi ^I	In-Sample	86.10	86.84	0.74	0.00
	Out-Of-Sample	78.88	78.91	0.03	0.46

Table 11: Average statistics of the models $PI^{[1]}$ (Eqn (6)), $CI^{[1]}$ (Eqn (12)), PI^I (Eqn (11)) and CI^I (Eqn (13)) in one-minute update frequency. The first and second column report the adjusted- R^2 of price-impact and cross-impact model, respectively. ΔR^2 is the increase in adjusted- R^2 . *p*-Value represents the probability of observing the increase in adjusted- R^2 under the null hypothesis of no increase.

B Cross-impact of multi-level OFIs on contemporaneous returns

We use the multi-level OFIs of multiple assets as candidate features to fit contemporaneous returns, as shown in Eqn (26). In this experiment, there are approximately 1,000 candidate features (100 stocks \times 10 levels) in each regression. We follow the same setting described in Section 3.3 and use LASSO to train this regression. Specifically, we use a 30-minute estimation window to estimate models and then apply the estimated coefficients to fit data in the next 30 minutes.

$$CI^{[10]} : r_{i,t}^{(h)} = \alpha_i^{[10]} + \sum_{m=1}^{10} \beta_{i,i}^{[10],m} ofi_{i,t}^{m,(h)} + \sum_{m=1}^{10} \sum_{j \neq i} \beta_{i,j}^{[10],m} ofi_{j,t}^{m,(h)} + \eta_{i,t}^{[10]}. \quad (26)$$

The results are summarized in Table 12 and reveal a similar conclusion as in Section 4. Additionally, compared with Table 5, we can conclude that CI^I and $CI^{[10]}$ have similar performances. Given the fact that the number of features used in CI^I is 1/10 of the number in $CI^{[10]}$, the advantages of integrated OFIs are once again reflected.

		PI (%)	CI (%)	ΔR^2 (%)	<i>p</i> -Value
[ofi ¹ , ..., ofi ¹⁰]	In-Sample	89.28	89.61	0.33	0.00
	Out-Of-Sample	84.21	83.35	-0.86	1.00

Table 12: Average statistics of the models $PI^{[10]}$, and $CI^{[10]}$ (Eqn (26)). The first and second column report the adjusted- R^2 of price-impact and cross-impact model, respectively. ΔR^2 is the increase in adjusted- R^2 . *p*-Value represents the probability of observing the increase in adjusted- R^2 under the null hypothesis of no increase. Note that here we use LASSO to fit $PI^{[10]}$ considering the multi-collinearity among multi-level OFIs; therefore, the results in first column are different from those reported in Table 1.

C Common factors of OFIs

Capponi and Cont [11] propose a two-step procedure to justify the significance of cross-impact terms. In the first step, they use ordinary least squares (OLS) to decompose each stock's OFIs into the common factor and the idiosyncratic components. In the second step, they regress returns of stock i on the common factor, its own idiosyncratic component and the idiosyncratic component of all other stocks. Nonetheless, Capponi and Cont [11] only consider the in-sample performance of their proposed model, and ignore the out-of-sample performance in the experiments. In addition, they employ OLS regression in both steps of their proposed pipeline, a technique unable to capture the potential sparsity of the cross-impact terms.

Motivated by this line of work, we follow their first step to obtain the market factor and residuals of each stock. However, we employ LASSO in the second step to testify the intraday cross-impact of the idiosyncratic OFIs. More specifically, as shown in Eqn (27), we first regress a stock's OFI ($\text{ofi}_{i,t}^{1,(h)}$) on the common factor of OFIs ($F_{\text{ofi},t}^{(h)}$), that is the first principal component of the multi-asset order flow imbalances, and obtain the idiosyncratic components ($\tau_{i,t}^{(h)}$) of the OFIs, for each individual stock.

$$\text{ofi}_{i,t}^{1,(h)} = \mu_i + \gamma_i F_{\text{ofi},t}^{(h)} + \tau_{i,t}^{(h)}. \quad (27)$$

Subsequently, we regress returns ($r_{i,t}^{(h)}$) of stock i against (i) the common factor of OFIs ($F_{\text{ofi},t}^{(h)}$), (ii) the idiosyncratic components of its own OFIs ($\tau_{i,t}^{(h)}$), and (iii) the idiosyncratic components of the OFIs of other stocks ($\tau_{j,t}^{(h)}, j \neq i$) via LASSO. Finally, we arrive at the cross-impact model in Eqn (28), denoted as CI^M .

$$\text{CI}^M : \quad r_{i,t}^{(h)} = \alpha_i^M + \beta_{i0}^M F_{\text{ofi},t}^{(h)} + \beta_{ii}^M \tau_{i,t}^{(h)} + \sum_{j \neq i} \beta_{ij}^M \tau_{j,t}^{(h)} + \eta_{i,t}^M. \quad (28)$$

We compare CI^M with a parsimonious model PI^M (Eqn (29)), in which only a stock's own OFI residual and the common order flow factor are utilized.

$$\text{PI}^M : \quad r_{i,t}^{(h)} = \alpha_i^M + \beta_{i0}^M F_{\text{ofi},t}^{(h)} + \beta_{ii}^M \tau_{i,t}^{(h)} + \epsilon_{i,t}^M. \quad (29)$$

We then train the PI^M and CI^M models on historical data, under the same setting as in Section 4.3. Similarly, we present the average R^2 values of PI^M and CI^M in Table 13. We observe small improvements (of only 1.13%) from PI^M to CI^M in in-sample tests. From considering Tables 5 and 13, we also observe that introducing the common factor leads to small changes in the model's explanatory power of price dynamics in the in-sample tests. However, both the price-impact and cross-impact models perform much worse in out-of-sample data, highlighting the importance of out-of-sample testing.

		PI^M (%)	CI^M (%)	ΔR^2 (%)	p -Value
ofi^1	In-Sample	71.38	72.51	1.13	0.0
	Out-Of-Sample	31.87	33.52	1.65	0.0
ofi^I	In-Sample	85.71	86.09	0.38	0.0
	Out-Of-Sample	46.27	46.82	0.55	0.0

Table 13: Average statistics of the PI^M (Eqn (29)) and CI^M (Eqn (28)) models. The first and second column report the adjusted- R^2 of the price-impact and cross-impact models, respectively. ΔR^2 is the increase in adjusted- R^2 . p -Value represents the probability of observing the increase in adjusted- R^2 , under the null hypothesis of no increase.

D Price-impact of multi-level OFIs on future returns

We use multi-level OFIs as candidate predictors to fit future returns $R_{i,t+1}$, as shown in Eqn (30). Given the fact that multi-level OFIs have a strong multicollinearity, we use LASSO to fit this regression. We follow the same setting described in Section 5. Specifically, we use a 30-minute estimation window to estimate models, and then make one-minute-ahead return forecasts.

$$\text{F-PI}^{[10]} : R_{i,t+1}^{(h)} = \alpha_i^F + \sum_{m=1}^{10} \left[\beta_i^{F,m} \text{ofi}_{i,t}^{m,(h)} + \gamma_i^{F,m} \text{ofi}_{i,t-1}^{m,(h)} + \theta_i^{F,m} \text{ofi}_{i,t-2}^{m,(h)} \right] + \eta_{i,t}^F. \quad (30)$$

The results in Table 14 provide evidence that the forward-looking price-impact model using multi-level OFIs significantly outperforms the forward-looking price-impact model with best-level OFIs or with integrated OFIs. These numerical results indicate that the integrated OFIs potentially lose valuable information in multi-level OFIs, which is important to forecast future returns.

		F-PI ^[1]	F-PI ^{I}	F-PI ^[10]
R^2 (%)	In-Sample	0.24	0.26	5.68
	Out-Of-Sample	-19.07	-17.62	-10.42
PnL (bps)	Forecast-implied	0.19	0.20	0.46
	Long-Short	0.10	0.12	0.51

Table 14: Average statistics of the models F-PI^[1] (Eqn (15)), F-PI ^{I} (Eqn (17)) and F-PI^[10] (Eqn (30)). The top panel reports the adjusted- R^2 on in-sample and out-of-sample data, respectively. The bottom panel reports the PnLs of forecast-implied portfolio and long-short portfolio, respectively. Note that the results about F-PI^[1] and F-PI ^{I} (the first two columns in this table) are the same as in Tables 6 and 9.